Universidade do Minho
Escola de Ciências

Joana Mendes Lopes de Melo

IL-27-regulated signalling pathways in Angiogenesis - possible role of MAPKinases.

Tese de Mestrado
Mestrado em Genética Molecular

Trabalho realizado sob a orientação de:
Professora Associada Katerina Tritsaris (Universidade de Copenhaga)

e co-orientação de:
Professora Auxiliar Paula Sampaio (Universidade do Minho)

Setembro de 2013

Declaração de reprodução

Nome: Joana Mendes Lopes de Melo

Endereço electrónico: jomlmelo@gmail.com

Número do Bilhete de Identidade: 13742613

Título tese de Mestrado:

IL-27-regulated signalling pathways in Angiogenesis - possible role of MAPKinases.

Orientadora:

Professora Associada Katerina Tritsaris (Universidade de Copenhaga)

Co-Orientadora:

Professora Auxiliar Paula Sampaio (Universidade do Minho)

Ano de conclusão: 2013

Designação do Mestrado: Mestrado em Genética Molecular

Universidade do Minho, ___/___/_____

_____

Joana Mendes Lopes de Melo

Acknowledgments

Until today many people crossed the road I have been taking, and influenced in my wishes and decisions. Looking back, I could not be more pleased with the professional I am becoming. Hopefully, I will continue to have the luck to meet new individuals along this road.

I must thank with my entire hearth, the opportunity given by Associate Professor Katerina Tritsaris to join the Angiogenesis Lab in the Faculty of Health Sciences, University of Copenhagen to complete my Master thesis. For all the optimism placed on me and for teaching me so much, my biggest appreciation.

I thank to Professor, Dr. Scient. Steen Dissing all the hours in the fluorescence microscope together and particularly all the patience teaching me how to use it. Additionally, I appreciate all the discussions about the work and the motivation always given.

I also have to thank to my lab colleagues, for such a good working environment, without them going to work every day would not be so pleasing. I specially acknowledge Sebastian, for the work we have done together, for what he taught me and for all the healthy discussions. Not forgetting all the Saturdays' keeping company to each other in the lab.

Moreover, I would like to recognize everyone in the building 12, 6th floor in the Faculty of Health Sciences, for receiving me in their home and teach me how to become a true Danish.

And naturally, family and friends, my biggest gratitude.

Vias de sinalização reguladas por IL-27 em Angiogénese – possível envolvimento de MAPKinases.

Angiogénese é o crescimento de vasos sanguíneos a partir de vasos pré-existentes. Sabe-se que é um processo envolvido em várias doenças inflamatórias, sobretudo devido a um desequilíbrio entre factores pro- e anti-angiogénicos no tecido inflamado. IL-27 é uma citocina produzida por células apresentadoras de antigénios, com propriedades pro- e anti-inflamatórias e potencial anti-angiogénico. Os sinalizadores de tradução e ativação de transcrição (STATs) são ativados por citocinas e alguns membros da família estão envolvidos em angiogénese, nomeadamente o STAT1. Quando STAT1 é fosforilado no resíduo de serina é induzida a expressão do factor regulatório de interferão-1 (IRF-1), pelo que se acredita que IRF-1 é necessário na angiogénese. Adicionalmente, sabe-se que as proteínas de ligação de guanilato (GBPs), são expressas devido à actividade de STAT1 e IRF-1. Foi também anteriormente sugerido o envolvimento das MAPKinases na angiogénese patológica, contudo a sua ligação ainda não é clara.

Com o objectivo de elucidar o mecanismo molecular na sinalização de IL-27 em células endoteliais, estudámos o mecanismo de fosforilação de STAT1 no resíduo de serina mediada pela IL-27, observando-se a consequente proliferação/sobrevivência e migração de células endoteliais de veia umbilical humana (HUVEC).

Os dados iniciais demonstraram que IL-27 leva à fosforilação do resíduo de serina em STAT1 e à expressão de IRF-1 em HUVEC. A inibição de SAPK/JNK reduziu a fosforilação de STAT1 no resíduo de serina, bem como a expressão de IRF-1, confirmando o envolvimento desta MAPK na fosforilação de serina em STAT1. Adicionalmente, verificou-se que a expressão de GBP1 e GBP2 é estimulada por IL-27 através da actividade de STAT1 e IRF-1. O papel das GBPs na angiogénese não foi esclarecido, estando a ser alvo de novos estudos.

O segundo objectivo desta tese era compreender o efeito biológico de IL-27. Desta forma, foi realizada a optimização de vários ensaios angiogénicos, *in vitro* e *in vivo*. Para o estudo *in vitro* da ramificação de vasos sanguíneos, a migração de células endoteliais e formação de tubos, foram utilizadas as técnicas “Endothelial Spheroid Angiogenesis Assay” e “Endothelial Tube Formation Assay”. Ambos os métodos optimizados revelaram ser ferramentas importantes para investigar sinalização intracelular, pois permitem a utilização de anticorpos, inibidores ou siRNA. Foi ainda testado o modelo de retina de ratinho, observando-se a redução do número de ramificações de vasos sanguíneos na retina, quando estimulados com IL-27. Este ensaio revelou resultados preliminares encorajadores.

Com este estudo temos agora uma melhor compreensão da sinalização de IL-27 em células endoteliais e o seu possível efeito biológico na angiogénese. Espera-se ainda contribuir para a identificação de novos alvos terapêuticos para angiogénese patológica. Contudo muitas questões foram levantadas, as quais serão futuramente objeto de estudo.

IL-27-regulated signalling pathways in Angiogenesis - possible role of MAPKinases.

Angiogenesis is the growth of new blood vessels from pre-existing vessels. It is a process known to be involved in many inflammatory diseases, mainly due to imbalance between pro- and anti-angiogenic factors in the inflamed tissue. IL-27, a cytokine produced by antigen-presenting cells with both pro- and anti-inflammatory properties, was previously demonstrated to have an anti-angiogenic potential. The signalling transducers and activators of transcriptions (STATs) are induced by cytokines and some of the family members take part in angiogenesis, namely STAT1. When STAT1 is serine-phosphorylated expression of interferon regulatory factor-1 (IRF-1) is induced, proposing IRF-1 association to angiogenesis. Additionally, is known that the guanilate-binding proteins (GBPs) are expressed due to STAT1 and IRF-1 activities. Also, it was previously suggested the MAPKinases involvement in pathological angiogenesis, but their connection is still unclear.

In order to clarify the molecular mechanism in IL-27 signalling in endothelial cells, was studied the mechanism of STAT1 serine phosphorylation mediated by IL-27, detecting subsequent proliferation/survival and migration of Human Umbilical Vein Endothelial Cells (HUVEC).

Initial data showed that IL-27 stimulated STAT1 serine phosphorylation and IRF-1 expression in HUVEC. Inhibition of SAPK/JNK reduced STAT1 serine phosphorylation and expression of IRF-1, thereby establishing the participation of this MAPK in STAT1 serine phosphorylation. Additionally, we observed that GBP1 and GBP2 expression was stimulated by IL-27 via STAT1 and IRF-1 activity. GBPs role in angiogenesis is now further explored.

The second aim of this thesis was to comprehend the biological effect of IL-27. Therefore, I started optimization of different *in vitro* and *in vivo* angiogenesis assays. To *in vitro* study of sprouting angiogenesis, migration of endothelial cells as well as tube formation, was used “Endothelial Spheroid Angiogenesis Assay” and “Endothelial Tube Formation Assay”. Both optimized assays are good tools for investigating intracellular signalling since the use of siRNA, inhibitors and antibodies is possible. The mouse Retina assay an *in vivo* angiogenesis model, showed a reduction in the number of branches in IL-27 stimulated eyes, providing encouraging preliminary results.

This study offered a better understanding of IL-27 signalling in endothelial cells and possible biological effect in angiogenesis. We hope to contribute for the identification of new therapeutical targets for pathophysiological angiogenesis. However, many new questions have been raised, which we aim to dissolve in the future.

Table of Contents

LIST OF ABBREVIATIONS

ANG II	angiopoietin II
ATP	Adenosine triphosphate
BrdU	Bromodeoxyuridine Assay
BSA	Bovine Serum Albumin
CAM	Chick Chorioallantoic membrane assay
cDNA	Complementary deoxyribonucleic acid
Ct	Cycle threshold
DMEM	Dulbecco's Modified Eagle's Medium
DTT	DL-Dithiothreitol
EBI3	Epstein-Barr virus-induced gene 3
EBM	Endothelial Basal Medium
ECM	Extracellular matrix
EDTA	Ethylenediamine Tetraacetic acid
EGF	Endothelial Growth Factor
ELISA	Enzyme-linked immunosorbent assay
ERK	Extracellular signal-regulated kinases
FBS	Fetal Bovine Serum
FGF	Fibroblast Growth Factor
GAPDH	Glyceraldehyde-3-phosphate dehydrogenase
GAS	IFN-γ activation site
GBPs	Guanylate-Binding Proteins
gDNA	Genomic deoxyribonucleic acid
GDP/GTP	Guanosine di/triphosphate
gp130	glycoprotein 130
HUVEC	Human Umbilical Vein Endothelial Cell
IAD1/2	IRF-associated domain 1/2
IFN	Interferon
IL-27	Interleukine-27
IP-10	interferon gamma-induced protein 10
IRF	Interferon Regulatory Factor
ISRE	IFN-stimulated response element
ISGF3	IFN-stimulated gene factor 3
JAK	Janus Kinase
MAP3Ks/MKKKs	MAP Kinase Kinase Kinase
MAPK	Mitogen Activated Protein Kinase
MEKs/MKKs	MAPK/extracellular signal-regulated kinase (ERK)-kinases
MMP	Matrix Metalloproteinase
MYD88	Myeloid Differentiation primary response gene 88
NGS	Normal Goat Serum
P5	Post-natal day 5
PBS	Phosphate Buffered Saline
PDGF	Platelet-derived Growth Factor
PFA	Paraformaldehyde
PIAS	Protein Inhibitors of activated STAT
PLF	Proliferin
PRL	Prolactin
Q-PCR	Quantitative- Polymerase Chain Reaction
RT	Reverse Transcription/ Reverse Transcriptase
SAPK/JNK	Stress-Activated Protein Kinases/Jun amino-terminal Kinases
SDS-PAGE	Sodium Dodecyl Sulfate-PolyAcrylamide Gel Electrophoresis
SH2	Src homology-2
siRNA	small interference ribonucleic acid
SOCS	Suppressor of Cytokine Signalling
STAT	Signalling Transducer and Activator of Transcription
TGF	Transforming Growth Factor
TLRs	Toll like receptors
TNFα	Tumor Necrosis Factor alpha
TRAF6	TNF-receptor-associated factor 6
UV	Ultra Violet
VEGF	Vascular Endothelial Growth Factor

Chapter I Background

1 Highlights in Angiogenesis

Angiogenesis is the growth of new blood vessels, from pre-existing vessels, which differs from vasculogenesis, the formation of new vessels in an avascular area[1] (Figure 1). In the healthy adult blood vessels are very stable and angiogenesis is rare, with the exception of events such as cyclical growth of vessels in the ovarian *corpus luteum* or during pregnancy[2]. However, angiogenesis is fundamental in several physiological and pathological conditions, for instance during development, modulation of the nervous system, tissue remodeling and in inflammation and cancer[3].

The formation of vessels is a complex process, which requires a precise balance between numerous stimulatory and inhibitory signals. Angiogenesis requires key regulators of vascular endothelial cells sprouting, like VEGF (vascular endothelial growth factor). Presence of VEGF leads endothelial cells begin to proliferate and migrate, originating the branching of new vessels. Other cytokines, such as Platelet-derived growth factor (PDGF) and angiopoietin-1 (ANG I) recruit mural cells around the endothelial channels[1,2,4]. Pericytes are specialized mesenchymal cells with finger-like projections that wrap around endothelial cells to provide structural support for newly formed blood vessels. In normal vessels they deliver paracrine support signals; they can produce low levels of VEGF, operating as trophic function in endothelial homeostasis and collaborate with endothelial cells to synthetize the vascular basal membrane[1,2,5].

Angiogenesis has been implicated in more than 70 disorders so far, and the list is ever growing. In many disorders, balance between stimulators and inhibitors is tilted, thereby regulating the angiogenic switch. The best-known conditions in which angiogenesis is switched on are malignant, ocular and inflammatory disorders, but many additional processes are affected, such as obesity, diabetes, multiple sclerosis, bacterial infections or autoimmune disease. In other diseases, such as ischemic heart disease or preeclampsia, the angiogenic switch is insufficient, causing endothelial cell dysfunction, vessel malformation or regression, or preventing revascularization, healing and regeneration[4].

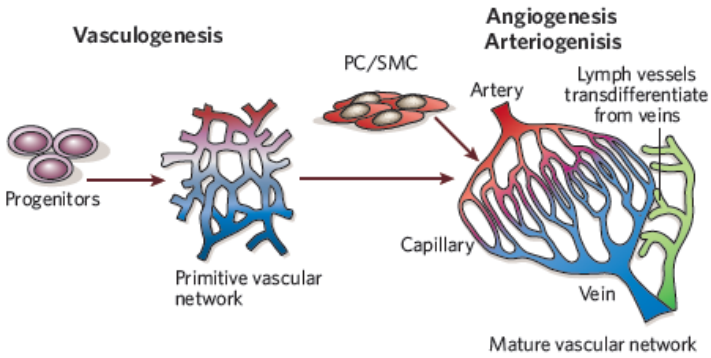

Figure 1: Development of the vascular system. Endothelial progenitor cells give rise to a primitive vascular network of arteries and veins, a process known as vasculogenesis. Subsequently, during angiogenesis, the network expands and an organized vascular network, with pericytes and smooth muscle cells covering the endothelial tubes, emerges. Figure withdrawal from Carmeliet (2005).

2 Tumor Angiogenesis

In 1971, Folksman wrote "survival and proliferation of cancer depend on angiogenesis". Tumors need microenvironment propitious to their growth. Initially, tumors are able to capture oxygen and nutrients by diffusion, however, they only grow until 2mm. In order to tumors to be able to increase in size it is necessary for them to have access to nutrients and oxygen, as well as to be able to excrete metabolic waste products and carbon dioxide. Therefore, a high number of vessels are needed[1,5].

Tumor vessels diverge from normal vessels. They are more dilated, tortuous and have low coverage of pericytes, which lead to hyperpermeability, higher interstitial pressure and lower blood flow[1]. Also, tumor vessels occasionally have cancer cells integrated into the vessel walls[6].

The angiogenic switch takes place in tumor development and can be regulated by countervailing factors, which either induce or inhibit angiogenesis. Recent studies, surprisingly shown that angiogenesis can be induced in the beginning of the multistage development of invasive cancers and is an important factor even in the microscopic premalignant phase of neoplastic progression. For this reason, angiogenesis has been considered one of the Hallmarks of Cancer[5].

There have been observed different grades of angiogenesis in distinctive tumors. Aggressive tumors, like pancreatic ductal adenocarcinoma, are hypovascularized, in contrast human renal carcinoma, is highly vascularized. These observations led to the hypothesis that

initial switch of angiogenesis is equal in different types of tumor, though this is preceded by variations in intensity of ongoing neovascularization[5].

Although tumor vessels present low coverage of pericytes, it has been found that these auxiliary cells are important in tumor neovasculature. The functional meaning of these cells was demonstrated by genetic and pharmacological perturbations, for example, through the inhibition of the PDGF receptor-β, expressed in tumor pericytes[7], leading to a reduced coverage of tumor vessels and consequently, compromises vascular integrity and function. It is also interesting to refer that pericytes present in normal vessels are not sensitive to pharmacological inhibition, which once more suggests differences in the regulation of normal and tumors vessels[5].

Already in 1971, investigators hypothesized that antiangiogenic therapy could be the key in human cancer treatment and began an active search for angiogenesis inducers and inhibitors. However, is now known that tumors vessel structure is thought to affect the drug targeting of cancer through angiogenesis[8]. Cells of innate immune system have a crucial role in pathological angiogenesis. Macrophages and neutrophils, among others, enter premalignant lesions and tumors and assemble themselves at the margins. Besides providing inducing signals for angiogenesis, they are able to protect the tumor vasculature from the effects of antiangiogenic drugs[5].

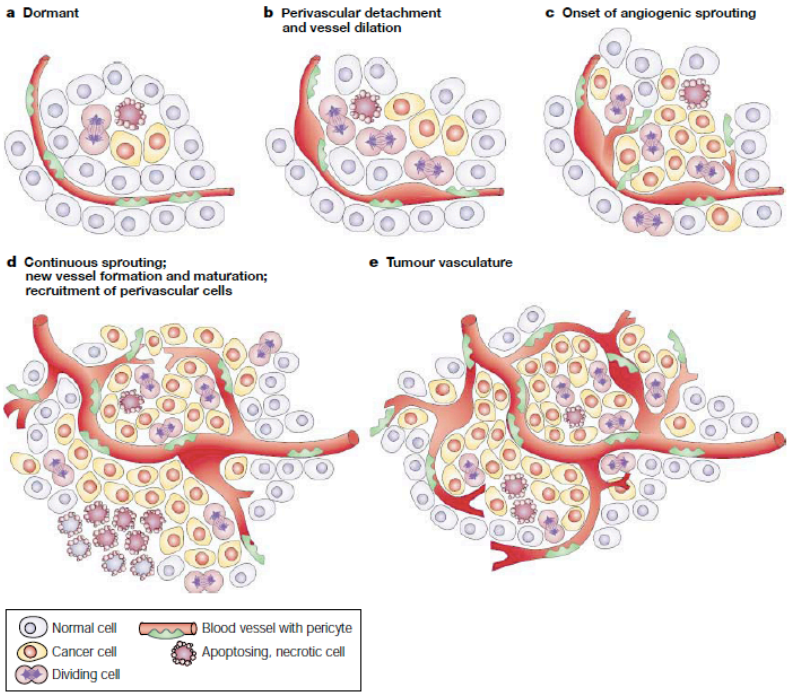

Figure 2: Onset of the angiogenic switch depends on the nature of the tumor and its microenvironment. The angiogenic switch ensures exponential tumor growth and begins with perivascular detachment and vessel dilation. Image withdrawal from Bergers and Benjamin (2003).

3 IL-27 in Angiogenesis

Interleukin 27 (IL-27) is a heterodimeric cytokine, belonging to IL-6/IL-12 family, comprising the cytokine subunit p28 and the soluble receptor Epstein-Barr virus-induced gene 3 (EBI3)[9,10]. Both subunits are required for secretion and normal function of IL-27[11].

The IL-27 receptor is composed of WSX-1 (also known as T cell cytokine receptor), a type I cytokine receptor, and glycoprotein 130 (gp130), a subunit used by several other IL-6 and IL-12 family members[9]. IL-27 intracellular signalling only occurs when IL-27 interacts with both subunits[12].

When IL-27 binds, the receptor is phosphorylated by Janus kinase 1 (JAK1), which is constitutively associated with WSX-1 via interaction with different cytoplasmic tyrosine residues[13]. The phosphorylated tyrosine residues function as docking sites for intracellular proteins, including the proteins of the signal transducers and activators of transcription (STAT) family[12] (Figure 3).

It is already known that IL-27 presents pro- and anti-inflammatory properties, although its contradictory effects are not fully understand. It appears that IL-27 signalling is dependent on the immunologic context[9]. Initially, IL-27 was reported to induce proliferation of naive $CD4^+$ T cells[11], as well as having T_H1-promoting abilities by up-regulating Interleukin 12 receptor b2 on naive T cells[14] and synergizing with IL-12 to induce production of interferon-γ (IFNγ)[15].

In vivo studies show that IL-27 also possesses immune-suppressive properties. IL-27R-deficient mice, comparing to wild type mice, developed severe disease in a model of experimental autoimmune encephalomyelitis. This effect was linked to the lack of IL-27 suppression of T_H17 cells in IL-27R-deficient mice[16].

Recently, IL-27 was found to be an important cytokine in angiogenesis. Previous findings, describe its direct role in angiogenesis reduction, however the mechanism of action is still unknown[10,17] . Yet, recently it was observed that IL-27 had anti-proliferative effect in lymphatic endothelial cells via JAK/STAT1 activation[18].

IL-27 is involved in the development of arthritis, as this was delayed in $IL\text{-}27R^{-/-}$ mice comparing with $IL\text{-}27R^{-/-}$ mice[19]. IL-27 also presents potent antitumor activity, which generally is mediated by $CD8^+$ T cells[10] and occurs by indirect mechanisms, like induction of NK cells or inhibition of angiogenesis through induction of IP-10 (interferon gamma-induced protein 10)

and IP-9. Lately, it was shown that IL-27 directly inhibits the proliferation of human melanoma cell lines, which express functional IL-27R[20].

Figure 3: Components of IL-27 and its receptor. In the presence of IL-27, the IL-27 receptor recruits Jak kinases, which in turn activate the STAT transcription factors. After being phosphorylated STATs enter the nucleus and modulate gene expression. Image withdrawal from Colgan and Rothman (2006)

4 Mitogen-activated protein kinases (MAPKs)

Mitogen-activated protein kinase (MAPK) signal transduction pathways are extensive mechanisms of eukaryotic cell regulation. Eukaryotic cells have multiple MAPK pathways, each preferentially recruited by different stimuli[21].

Mammalian MAPK pathways act through diverse receptor families, including hormones and growth factors that exert their action through receptor tyrosine kinases [e.g., insulin, epidermal growth factor (EGF), platelet-derived growth factor (PDGF), and fibroblast growth factor (FGF)] or cytokine receptors (e.g., growth hormone). MAPKs can also be activated by vasoactive peptides that act through G protein-coupled receptors (e.g., ANG II, endothelin) or throught transforming growth factor (TGF)-related polypeptides, acting through Ser-Thr kinase receptors. Environmental stresses also lead to MAPK activation, such as osmotic shock, ionizing radiation and ischemic injury. In turn, MAPK pathways exert a profound effect on cell physiology, namely on gene transcription, protein synthesis, cell cycle machinery, cell death, and differentiation[21].

MAPK include ERK, p38 and SAPK/JNK. The extracellular signal–regulated kinases (ERKs) was the first mammalian MAP Kinase to be identified, followed by the stress-activated kinases SAPK/JNK and p38. ERK is activated in response to cell cycle progression or cell

differentiation, while both SAPK/JNK and p38 are induced by stress stimuli, for instance, osmotic stress or UV radiation[21].

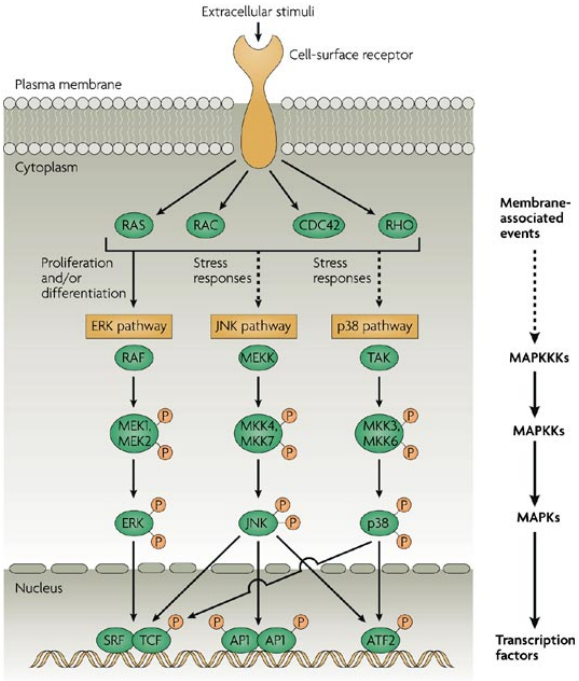

Figure 4: MAPKs pathways. Image Withdrawal from Liu et al. 2007.

All MAPKs are activated by simultaneous Tyrosine and Threonine phosphorylation within a conserved Thr-X-Tyr motif in the activation loop of the kinase domain subdomain VIII. MAPK phosphorylation and activation are catalysed by a family of dual specificity kinases referred to as MAPK/extracellular signal-regulated kinase (ERK)-kinases (MEKs or MKKs). These are themselves regulated by Serine/Threonine phosphorylation, also within a conserved motif in kinase domain subdomain VIII, which is catalysed by any of the protein kinase families referred to as MAPK-kinase-kinases (MKKKs or MAP3Ks)[21].

To date several anti-angiogenic compounds have been reported to inhibit the activation of ERK1/2 signal cascade induced by VEGF (vascular endothelial growth factor) and bFGF (basic fibroblast growth factor), indicating an involvement of ERK1/2 in angiogenesis. p38 was likewise reported to be involved in regulating VEGF-induced HUVEC cell migration, having an important role in angiogenesis. Furthermore, SAPK/JNK was described having an antiangiogenic role via inhibition of VEGF secretion and metalloproteinase (MMP) from HUVEC cells. Active MAPKs have been detected in many diseases involving angiogenesis like tumor progression and metastasis, diabetic retinopathy and age-related macular degeneration, suggesting that MAPKs take part in angiogenesis-associated diseases[22].

4.1 P38

P38 belongs to mammalian stress-activated MAPK family and was originally described as a 38kDa polypeptide, which were regulated by Tyrosine phosphorylation. After the p38 alpha isoform was discovered this mammalian MAPK showed high homology to HOG1, the

osmosensing MAPK of S. cerevisiae, and like this, contained the conserved sequence Thr-Gly-Tyr[21].

To date, four isoforms of the p38 family, namely p38α, p38β, p38γ, and p38δ, were identified and are encoded by distinct genetic loci, but all share the common Thr-Gly-Tyr motif in kinase subdomain VIII[23,24]. Usually all isoforms are inactive in the cytoplasm, but after phosphorylation are translocated to the nuclei, where they phosphorylate diverse substrates[24]. Among all p38 MAPK isoforms, p38α is the best characterized and it is expressed in most cell types, while p38β is present mostly in the brain, p38γ is most significantly expressed in skeletal muscle and p38δ in endocrine glands[25,26]. The p38 MAPK subfamily can be divided into two distinct subsets, p38α and p38β on the one hand and p38γ and p38δ on the other. P38α and p38β share a similar amino-acid sequence, being 75% identical[25]. In addition, three-dimensional structure of p38β is very similar to that of p38α, with some differences in the orientation of the N- and C-terminal domains affecting the size of the p38β ATP-binding pocket[26]. p38γ and p38δ are more identical to each other, about 70% identical[25].

P38 pathway is commonly known for tumor suppression, regulation of cell survival and proliferation, differentiation and apoptosis[24]. The p38 signalling pathway is activated by several stimuli and stresses, like environmental stress, bacterial lipopolysaccharide, inflammatory cytokines, heat shock, UV light, hypoxia, ischemia[23,24]. Its activation is relative to pro-apoptotic stimuli, but the biological outcome is highly dependent on cell type or context[23].

P38 is regulated upstream by MKK3 and MKK6[27]. Both MKK3 and MKK6 are highly selective for p38, MKK6 can phosphorylate all p38 family members, whereas MKK3 can not activate p38β[26,28]. In response to most stimuli p38α is activated by MKK3 or MKK6, although in some conditions, such as ultraviolet radiation, MKK4, an activator of JNK, may contribute to the p38α activation[25]. However, p38 isoforms are also capable of activating themselves through autophosphorylation, thereby being completely independent of MAPKKs[24].

Activation of p38 MAPK occurs within minutes and is transient, suggesting that p38 MAPK functions as a biological switch, probably downregulated under basal conditions and during adaptation. MAPK phosphatases reverse the phosphorylation and MAPK return to their inactive state[25]. Studies reveal that p38 is activated by several growth factors including FGF-2[27]. When FGF-2 induces activation of p38 activity in endothelial cells, MKK3/6 negatively

regulates the endothelial cell differentiation through a decrease in expression of proteins involved in differentiation, like Jagged1 (Notch ligand)[23].

4.2 JNK

The JNK is one of the major MAPK pathways[29]. The indication that cells possess several MAPK pathways arises after ERK discovery, since injection of cycloheximide into rats triggered a new Ser/Thr kinase activity with the ability to phosphorylate microtubule-associated protein-2 (MAP2). JNK was found to be a 54kDa polypeptide, and for that was given the initial name of p54. Similar to ERK, was inactivated with Tyr or Ser/Thr phosphatases, indicating that it required simultaneous Tyr and Ser/Thr phosphorylation for activation[21]. Afterwards was discovered the ability for p54 to phosphorylate the c-Jun transcription factor at two sites (Ser^{63} and Ser^{73}) in a substantially higher rate than observed for the ERKs[21].

JNKs were isolated and characterized as stress-activated protein kinases grounded on their activation in response to inhibition of protein synthesis[29]. JNK is an extremely regulated and complex pathway and is influenced by 13 different MKKKs. Generally, it is identified by two names: stress-activated protein kinase (SAPK) due to their regulation by environmental stress and inflammation and c-Jun NH2-terminal kinase (JNK) referring to the phosphorylation by these kinases of the c-Jun NH2-terminal trans-activation domain affinities[21].

The JNK proteins are encoded by three genes (JNK1-3), and alternative splicing gives origin to at least 10 different isoforms[29]. Splicing within the catalytic domain results in type 1 and type 2 SAPKs (b and a JNKs, respectively), while splicing at the COOH terminus bears 54kDa (p54) and 46kDa (p46) polypeptides (type 2 and type 1 JNKs, respectively. The exact significance of the COOH-terminal isoforms is still not clear, but was already observed that type 1 and type 2 kinases differ in their substrate binding affinities[21]. The JNK1 and JNK2 are present in nearly all cells, yet JNK3 is mostly present in the brain[29].

JNKs are triggered in response to growth factors, proinflammatory cytokines, microbial components, and a variety of stresses, including oxidative stress[30]. They are important in controlling programmed cell death[31], as well as cell proliferation, migration, survival, and cytokine production[30].

JNK has previously linked to cancer, were inhibition of JNK enhanced chemotherapy effect in fighting tumor growth[31]. Also was recently shown that JNK1 is a critical factor for

VEGF production caused by hypoxia in retina, stimulating hypoxia-induced pathological angiogenesis[30].

4.3 ERK

Human ERK1 and ERK2 share about 84% similarity and most of the known functions, since all the cellular stimulus lead to parallel activation of both ERK1 and ERK2. Only recently, using gene ablation studies was possible to understand differential functions for these protein kinases. Has shown that ERK1 gene is not necessary for mice development. ERK1-deficient mice were viable, fertile, and of normal size, yet, it appears to play an important role in thymocyte development. ERK2 gene ablation led to embryonic death. It was found that development of placental vasculature is severely impaired in ERK2-deficient mice and that embryonic trophoblast development is impaired in ERK2-deficient mice[32].

ERK1 and ERK2 are widely expressed and participate in the Ras-Raf-MEK-ERK signal transduction cascade. This signalling pathway exert function related with cell adhesion, cell cycle progression, cell migration, cell survival, differentiation, metabolism, proliferation, and transcription[32]. Many different stimuli activate the ERK1 and ERK2 pathways, like growth factors, cytokines, virus infection, transforming agents, and carcinogens[31].

There are common oncogenic mutations that convert Ras to an activated oncogene in many human tumors[31], and this occurs in about 30% of all human cancers[32]. Oncogenic Ras persistently activates ERK1 and ERK2 pathways, contributing to increased proliferation of tumor cells. Therefore, inhibitors of ERK pathways are in clinical trials as potential anticancer agents[31]. Activating mutations in Raf occur in near 7% of all human cancers[32].

Recently, there are reports of several anti-angiogenic compounds capable of inhibiting activation of ERK1/2 signal cascade induced by VEGF and bFGF, indicating that ERK pathway might play a role in angiogenesis[22].

5 STAT proteins

Signal Transducer and Activator of Transcription (STAT) family is a group of transcription factors that are present in their inactive form in the cytoplasm, but move to the nucleus once they are activated. The first two members of the family, STAT1 and STAT2 were

identified more than a decade ago and were acknowledged as mediators of cellular response to interferons[33].

There are seven different STAT proteins, which can be divided in two main groups. STAT2, 4 and 6 are activated by a low number of cytokines and have a role in T-cells development and IFNγ signalling. STAT1, 3, 5a and 5b are activated in several different tissues, with an important role in cell-cycle progression and apoptosis. This last group also contributes to oncogenesis, which makes them extensively studied[34].

All STATs proteins share similar structural domains (Figure 5). The NH2-terminal domain highly conserved and mediates protein-protein interactions and stabilizes binding of two STAT dimers to DNA; as for the coiled-coil domain, this establishes association with other important proteins. The DNA-binding domain determines the specificity of each STAT protein to DNA and the linker domain establishes a bridge between DNA-binding and Src-homology-2 (SH2) domains. The SH2 domain is necessary for dimerization of two STAT monomers through phosphotyrosine interactions. In this domain there is a critical tyrosine residue, when STAT proteins are phosphorylated, the SH2 domain binds to another STAT protein. At the C-terminal of STAT, there is the Transcriptional activation domain (TAD), which interacts with the transcriptional machinery to promote gene expression. Inside this domain some STAT proteins have a conserved serine, another phosphorylation site that regulates transcriptional activity[34,35].

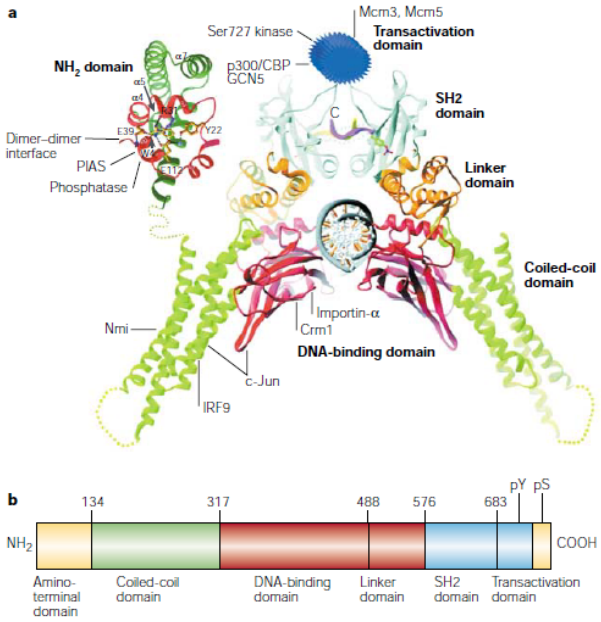

Figure 5: Signal Transducer and Activator of Transcription structure. a: STAT domain structure and protein biding sites. b: STAT domains and phosphorylation sites. Image withdrawal from Levy and Darnell (2002)

Currently several mechanisms to induce tyrosine phosphorylation in STATs are known (Figure 6). The well-known JAK-STAT pathway is initiated by a cytokine, which binds to a cell-surface cytokine receptor. Commonly, the intracellular domains of these receptors are

associated with tyrosine kinases from the Janus kinase (JAK) family. The receptor-associated JAKs phosphorylate the cytoplasmic tails of the cytokines receptors upon activation, leading to recruitment and after that phosphorylation of STATs proteins. JAKs are also involved in phosphorylation of STATs via G-protein coupled receptors. Usually hormones or chemokines bind to this type of receptors and phosphorylation of STATs occurs. There is a third mechanism of STATs activation, which involves Growth-factor receptors; these possess an intrinsic tyrosine kinase activity[33,34].

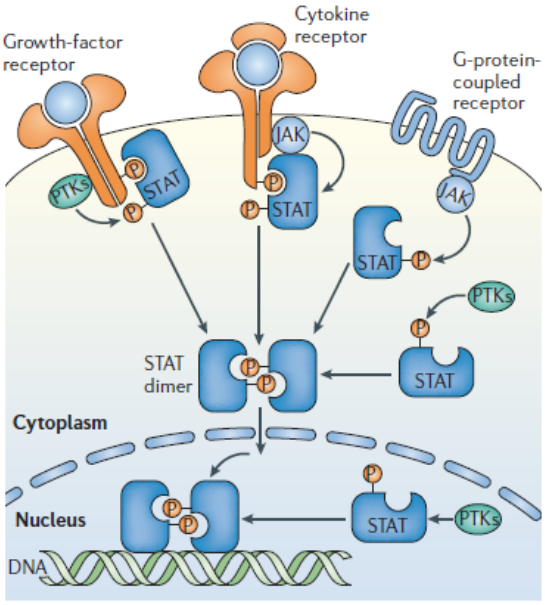

Figure 6: STAT tyrosine phosphorylation by receptor and non-receptor kinases. There are multiple mechanism used by JAKs or other PTKs (protein tyrosine kinases), which are intrinsic in the receptor or present in cytoplasm or nucleus. After tyrosine phosphorylation, there is STAT dimerization and binding to DNA. Image withdrawal from Reich and Liu (2006)

Via the SH2 domain, the STAT proteins become phosphorylated themselves by Jak on the C-terminal tyrosine residue, which leads to dissociation from the receptor and enables the phosphorylated STAT proteins to form homodimers or heterodimers. STAT dimerization is followed by translocation to the nucleus, where the STAT dimer binds to specific promoter elements in the DNA and activates gene transcription. Different STAT proteins are able to activate transcription of different genes, since they can recruit distinct co-activators, and so bind to different DNA sequences[36].

A second phosphorylation of STAT proteins can take place on a serine residue in the C-terminal end. In both STAT1 and STAT3, this serine residue is found in position 727 within a conserved proline-methionine-serine-phenylalanine (PMSP) motif. Several results suggest that the phosphorylation of this serine enhances the activity of STAT proteins, since mutation of the serine to alanine results in a reduced cytokine-stimulated transcription activity[37].

Serine phosphorylation of STATs can occur through different signal transduction pathways, depending on the signal received by the cell. Until now, the involvement of ERK pathway in serine phosphorylation of STAT3 by receptor tyrosine kinases and IL-2 has been

reported[38,39], as well as ERK involvement in serine[725] phosphorylation of STAT5[40]. ERK2 was also connected to serine phosphorylation of STAT1[41]. SAPK/JNK pathway so far is only linked to STAT3 serine phosphorylation caused by stress signals, like UV irradiation and hyperosmolarity or by inflammatory signals, like TNFα[42,43]. STAT1 serine phosphorylation, also in situations of stress and inflammation seems to occur via p38[44]. However, further studies are required to fully understand STATs serine phosphorylation.

STATs proteins have an important role in immune responses. STAT1 knockout mice are highly susceptible to infection by microbial agents and viruses, since they have compromised response to IFNs. Animals lacking STAT3 dies in an early embryonic state, indicating that this protein might have a crucial role in normal development[33]. In addition, STAT1 and STAT3 have both been implicated in the biological functions of the vasculature. STAT1 is reported to mediate anti-angiogenic signalling of IFNγ in human umbilical vascular endothelial cells (HUVEC)[45] and STAT3 to mediate pro-angiogenic signaling[46].

5.1 Regulation of STAT activity

STATs proteins are temporarily activated. After a few hours, activating signals decay and STATs are exported from the nucleus back to cytoplasm[34].

To decrease STAT DNA-binding activity dephosphorylation of STAT and/or dephosphorylating of the binding sites on the cytokines receptor is required. In both cases this is occurs by action of protein phosphatases (Figure 7a and c)[34,47]. SHP-2, a protein phosphatase, was identified as a regulator of STAT1 in the nucleus, dephosphorylating both Tyrosine[701] and Serine[727] [48].

STATs proteins are also regulated by the suppressor of cytokine signalling (SOCS) protein family (Figure 7b)[34]. SOCS proteins are generally expressed at low levels in unstimulated cells and become rapidly induced by cytokines to inhibit STAT signaling[49]. Interestingly, some SOCS proteins are transcriptionally regulated by STAT activity, working as a negative feedback loop[34].

SOCS proteins via the SH2-domains, to phosphorylated tyrosine residues on the cytoplasmic part of receptor chains or to phosphorylated proteins associated with the receptors, such as Jak proteins[50].

Moreover, protein inhibitors of activated STATs (PIAS) are thought to inhibit STAT signalling by blocking STAT DNA-binding (Figure 7d) PIAS1 and PIAS3 interact with STAT1 and STAT3, respectively, only when their tyrosines are phosphorylated. There are also natural occurring truncated forms of STATs, which act as dominant-negative proteins, either forming dimers with wild-type STATs (Figure 7e) or binding to DNA as non-functional protein[34].

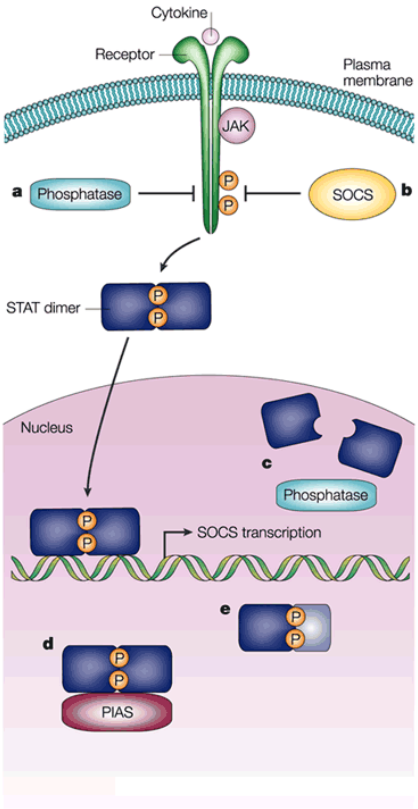

Figure 7: Regulation of JAK-STAT signalling

(A) Cytoplasmic phosphatases regulate STAT signalling by dephosphorylation of the phosphorylated tyrosine residues in the cytoplasmic tails of the receptor to prevent STAT-binding to the receptor.

(B) SOCS proteins regulate STAT signalling by binding to the phosphorylated tyrosine residues in the receptor and inhibiting the enzymatic activity of Jak.

(C) Nuclear phosphatases regulate STAT signalling by dephosphorylation of STAT proteins, which results in STAT dimer dissociation.

(D) PIAS proteins regulate STAT signalling by binding to STAT dimers in the nucleus and blocking their DNA-binding ability.

(E) Endogenous truncated STAT proteins regulate STAT signalling by forming dimers with phosphorylated STAT proteins and functioning like dominant negative proteins.

Figure withdrawal from Levy and Darnell (2002)

5.2 STAT5

STAT5a was identified originally as a transcription factor that regulates the β-casein gene in response to prolactin (PRL), however it is now known that it is also activated by numerous cytokines and growth factors[51]. STAT5a and STAT5b are two members of the STATs family, which share 96% identity and diverge basically in the C-terminal transactivation domain[52]. Their expression pattern is also different, STAT5a is mainly present in the mammary gland, but STAT5b is predominantly expressed in liver[51].

STAT5 has been implicated in several signalling events associated to the immune system, mammary epithelial cells or hepatocytes[52]. In addition, it has been found to be involved in a few malignances. In the case of hematopoietic cells, STAT5 regulates apoptosis, proliferation and cell cycle progression[51].

Initial studies suggested that STAT5a and STAT5b possessed similar functions, however, after STAT5a and STAT5b single knockout mice showed different phenotypes. Knockout of STAT5a results in compromised mammary gland development owing to loss of prolactin response. Knockout of STAT5b leads to sexually dimorphic growth retardation. Moreover, STAT5a/b double knockout showed a severe phenotype, many mice died a few days after birth were infertile and presented compromised immune system, with absence of NK-cells and a reduced number of B-cell precursors[51]. Yet, is interesting to see upon STAT5 deletion that many cells appear to adapt instead of undergoing apoptosis. Other members of the family are recruited to their receptor-binding sites, in fact, deletion of STAT5 from hepatocytes caused an abnormal activation of both STAT1 and STAT3[52].

STAT5 has recently been implicated in Angiogenesis. Researchers have reported that STAT5 and to a minor degree STAT1 were activated by FGF2 and FGF8b in mouse brain endothelial cells, inducing migration, invasion and tube formation in collagen. However STAT5 had no effect on proliferation[53]. The same group further investigated, and discovered that STAT5 is necessary on secretion of proliferin (PLF, an autocrine factor from the prolactin family) for STAT5-mediated angiogenesis[54].

6 IRF-1

The first Interferon-Regulatory Factor (IRF-1) was identified in 1988, and since then, nine members of the family have been recognized[55].

Structurally, all members present a well-conserved N-terminal DNA-binding domain (DBD) that recognizes a DNA sequence known as IFN-stimulated response element (ISRE). It is characterized by a set of five tryptophan-rich repeats. The IRF C-terminal domain is less conserved among the members of this family. This domain is responsible for the specificity of each member, since it mediates interactions with other proteins and co-factors. Within the C-terminal there is an IRF-associated domain 1 (IAD1, in IRF members 3-9) and IAD2 (only shared by IRF-1 and 2), necessary for DNA binding[55] (Figure 8).

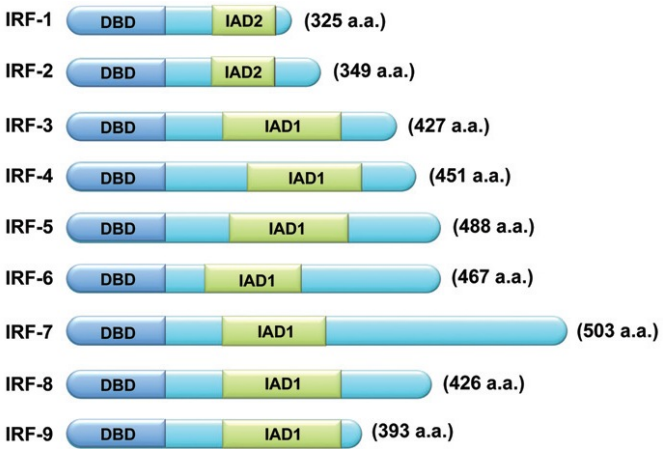

Figure 8: Illustration of human IRF family members. Image withdrawal from Yanai *et al* (2012).

The IRF family members share several functions. In host defence, essentially all IRFs mediate both activation and reduction of immune response. In immune cell differentiation regulation is mediated by IRF-1, -2, -4 and -8. In cell growth and cell death is again regulated by all IRFs[55]. These overlapping functions are due to the common ability that IRFs share to interact with MYD88 (Myeloid Differentiation primary response gene 88) and TRAF6 (tumor-necrosis-factor (TNF)-receptor-associated factor 6), two adaptor proteins involved in proper response of TLRs (Toll-like receptors)[56].

IRF-1 is known to be strongly induced by IFNγ. It has a short half-life of 30 minutes and is cell cycle regulated, presenting high levels in serum-starved G0. Also mRNA levels of IRF-1 increase before and after S phase[57].

IRF-1 is constitutively localized in the nucleus and its most important role is the ability to activate transcription of specific promoters. Its activity is regulated in several different ways, primarily at transcriptional level. It is not certain that IRF-1 regulation is dependent of phosphorylation and more observations are necessary. It is known a negative feedback mechanism for IRF-1 activity. IRF-1 activates IRF-2 promoter, which in turn inhibits IRF-1 transcription[57].

Currently several IRF-1 target genes have been identified, though not all functions are known. Original, IRF-1 was identified as a DNA-binding protein of positive regulation in the IFNβ promoter, which is responsible for antiviral response. Now IRF-1 is known to have a role in apoptosis, through regulation of Caspase 1 and 7 transcription, antiproliferative activity, through induction of the $p21^{WAF1/CIP1}$ promoter or antiviral activity (although to be confirmed) through Guanylate-binding proteins (GBPs) activation[57].

7 GBPs

The Guanylate-binding proteins (GBPs) were first identified in the late 1970s. Based on the crystal structure of GBP1 and on biochemical considerations[58] was proposed they belong to the family of large GTPases, together with Dynamin and Mx[59]. The family of large GTPases is characterized by high molecular mass, low affinity to the substrate GTP, high GTPase activity, ability to dimerize/oligomerize in the presence of substrate and after substrate binding are capable of self-assemble and stimulate their own activity[59].

The GBPs are the most distantly related members and have a variety of structural and biochemical properties that make them unique within this larger community. GBP family comprises proteins of 67kDa induced by both type I and II IFNs[60]. So far, in humans is known 7 GBPs[61]. Their main property is to hydrolyze GTP to both GDP and GMP[60], however, only hGBP1 and hGBP2 have experimentally exhibit GTPase activity. HGBP1 has GMP has major product of the reaction, while hGBP2 presents GDP as major product[62].

Initial studies showed two important promoter elements, after GBPs induction by IFN-α and IFN-γ, the ISRE and IFN-γ activation site (GAS). In some cells, hGBP1 induction by IFN-α/β is rapid, transient and does not require de novo protein synthesis. This occurs through the activation of the transcription complex IFN-stimulated gene factor 3 (ISGF3), a complex formed by STAT1, STAT2, and IFN regulatory factor-9 (IRF-9) that binds to the ISRE. Induction of hGBP1 by IFNγ is also rapid but more robust and more sustained than observed for IFNα/β. In fibroblasts, the ISRE site is sufficient for IFNγ induction of hGBP1. During IFNγ treatment, it is the transcription factor IRF-1 that binds to the ISRE element and the GAS site is bound by STAT1 homodimers[60]. Not all hGBPs have both GAS and ISRE elements in their promoter so it remains unclear whether all of the hGBPs are induced by either type I or type II IFNs. However, hGBPs 1 through 5 can be induced by IFN-γ in cultured endothelial cells. In addition, hGBP1, 2, and 3 are induced by IL-1β and TNF-α[61]. More recently, GBPs were shown to be inducible by other cytokines as well[60].

The addition of isoprenoid lipids to the carboxy-terminial of the protein was shown to have profound consequences. The CaaX motif is the recognition sequence for either farnesyl transferase or geranylgeranyl transferase I. Isoprenylation is important in targeting of proteins to intracellular membranes, as observed for Ras, and for protein-protein interactions[60]. Fairly surprisingly, whether isoprenylated or not, the GBPs are predominantly cytosolic in localization[60], with only a relatively small portion of the protein associated with

membranes. The ability to associate with membranes is an additional property that GBPs shared with other members of the family of large GTPases[61]. In specific hGBP-1 is present in the cytoplasm and can temporarily translocate into the Golgi apparatus, while hGBP2 is present in the cytoplasm and in the nucleus also translocating into the Golgi apparatus in the presence of IFNγ[63].

HGBP1 is until know the best studied GBP, and its structure has already been analysed. *In vivo*, hGBP1 expression is nearly exclusively related with endothelial cells[63].

There are several known GBPs functions, like antiviral and antimicrobial activity, inhibition of proliferation in endothelial cells and inhibition of expression of Metalloproteinase-1 by hGBP1 in endothelial cells[61]. The antiviral activity observed for GBPs is significantly lower than the one observed for the antiviral protein Mx, suggesting that the principal function of GBPs is not antiviral activity[60].

Previous studies shown that treatment with IFNγ, TNFα or IL-1β in endothelial cells could inhibit proliferation stimulated by growth-factor, through hGBP1 induction, but surprisingly not requiring GTPase activity[60].

A crucial feature of angiogenesis is invasion of endothelial cells into the extracellular matrix. This is a multistep process in which cell motility is connected to proteolysis. Angiogenic proteolysis is dependent on matrix metalloproteinases (MMPs), a family of zinc-dependent endopeptidases. The release of MMP-1 by endothelial cells is crucial for angiogenesis and cleavage of collagen type I, a substrate of MMP-1, is required for endothelial cell invasion into the ECM and for vessel formation *in vivo*[58]. MMP-1 is downregulated by GTPase activity of hGBP1, inhibiting invasion of endothelial cells and their ability to form tubes in a three-dimensional matrix containing collagen I[60]. Golgi translocation is not required for neither of these hGBP1 functions in endothelial cells, but may regulate additional roles, which have to be elucidated in future studies[63].

The capability of hGBP1 to inhibit both invasion (via its GTPase activity) and proliferation (via its helical domain) establishes GBP1 as a key intermediary of the anti-angiogenic effects of inflammatory cytokines in endothelial cells[58].

8 Angiogenesis Assays

In the previous 40 years the angiogenesis study has grown dramatically, specifically due to the acknowledgment that angiogenesis, besides being crucial in normal development processes, is a mark of more than 50 different pathologies[64].

Physiological angiogenesis is a sequence of highly organized events, starting with vascular initiation and formation, followed by maturation, remodelling and regression of vessels. However, in contrast to physiological angiogenesis, pathological angiogenesis is not properly regulated and most vessels do not maturate, remodelate or regress. It is therefor mandatory to study each angiogenic process with accuracy and in detail, in order to develop new therapeutic strategies[64].

A central problem for angiogenesis studies is to choose the most suitable assay to evaluate the efficacy of pro- and anti-angiogenic agents, and eventually to identify potential targets within the angiogenic process[65]. The ideal angiogenesis assay is rapid and reproducible with automated computational quantification[64]. However, we still lack an *in vitro* assay which gives all the answers, it is therefore required to use a combination of different *in vitro* assays, which can answer to different steps in the angiogenesis process and eventually identify the molecular mechanisms underlying it.

8.1 *In vitro* angiogenesis assays

In vitro assays have several advantages. They are often more easy to perform and to quantify, than *in vivo* studies. In addition, they are valuable tools in the initiation of any study providing initial information. But extreme caution is required when deducing results[65].

Cell proliferation assays are usually used for their high reproducibility and precise quantifiable data. Cell proliferation can be measured as the rate of cells dividing or as the final number of cells. Currently, it is possible to measure this parameter in several different ways, we can for instance count the net cell number by using a heamocytometer or a coulter counter. Yet, both bring disadvantages, the heamocytometer requires a high number of cells, while the results from the coulter counter might not always be due to cell proliferation, a decrease in cell number may be a result from cell death. MTT ([3-(4,5-dim- ethylthiazol-2-yl)-2,5-diphenyltetrazolium bromide) is another common method. The yellow tetrazzolium salt after mitochondrial cleavage produces blue formazan crystals, which accumulates in living

cells. This method brings rapid results, but some chemical reagents can interfere with the enzyme responsible for formazan production without changing the cell number. In addition, this method measures mitochondrial activity, which does not mean a change in cell number[64].

Cell proliferation can also be measured through DNA synthesis and Bromodeoxyuridine (BrdU) method has started to be used. BrdU competes with thymidine for incorporation in the DNA during S-phase of cell cycle. This is a colorimetric assay, easily detected by an ELISA micro-plate reader[64] that can be used for measuring the proliferation rate.

In vitro angiogenesis assays, among many others, also comprise Cell differentiation assays. These are used to measure formation of capillary-like structures that are representative of the later stages of angiogenesis[64]. These types of assays are used extensively to test new compounds with pro- or anti-angiogenic effect[65].

Embedding cellular aggregates in a matrix, like collagen, can lead to radial capillary sprouting. The spheroids are produced with a precise number of cells, which makes the assay possible to be standardized. The main advantage of this assay is the possibility to observe sprouting angiogenesis through invasion. This ultimately leads to formation of a complex capillary three-dimensional network, if the spheroids are allowed to proceed for several days. In summary, this assay appears to be the closest representation of angiogenic invasion, already proven to be useful for screening of pro- and anti-angiogenic factor. Moreover, it is a simple method with high reproducibility[66].

Tube formation assays are some of the most specific tests that measure the ability of endothelial cells to form three-dimensional structures[65]. Essentially, endothelial cells are seeded on top or embedded in a gel matrix, consisting of collagen, fibrin or Matrigel. After attaching to the matrix, they migrate towards each other, align and form tubes. This assays shows considerable flexibility[67].

Matrigel, a compound derived from the mouse Engelbreth-Holm-Swarm sarcoma, has proven to be the most powerful matrix for this assay. Afterwards, it has become available a growth factor reduced Matrigel, where the levels of cytokines and growth factors are diminished to circumvent problems associated with over-stimulation of endothelial cells[64], thereby reducing background.

One advantage is the possibility to quantify the extent of tube formation, mainly using four variable, average tube length, number of tubes, tubes area and branch points. In addition, image analysis software's that help performing a reliable quantification are emerging[64]. The tube formation assay, besides being a reliable method, is also more comprehensive than many other *in vitro* assays, and for that preferred for screening angiogenic regulators[67].

It is also possible to perform tube formation assays co-culturing endothelial cells with stromal cells, like fibroblast, smooth muscle cells or blood vessels explants, allowing a closer resemble to capillary bed in vivo. Yet, is of notice that co-culturing cells makes the assay time consuming and more difficult to quantify[64]. It is therefore necessary to consider which are the most appropriate assays to use.

Observations tell that an angiogenic agent that exert an effect *in vitro*, may not exhibit any activity *in vivo*, being also true the opposite, when certain compounds show more pronounced activity *in vivo*. Therefore, it is necessary to validate all results previous observed in *in vitro* assays, with *in vivo* angiogenic assays[64]. *In vivo* experiments allow for more realistic observations of the complex nature of the angiogenic response[65].

8.2 *In vivo* angiogenesis assay

There are many *in vivo* angiogenesis assays emerging, mainly due to differences in interpretation and comparison of *in vitro* assays, between research groups. So far, many different animal models are used, like chick egg or zebrafish, both simple and economical. However, care must be taken with these animal models[64]. To perform the Chick Chorioallantoic membrane assay (CAM) several limitations are necessary to take in account. CAM is well vascularized, which leading to a high background. Also cutting the shell may induce an inflammatory response, which itself induces angiogenesis. In the zebrafish model, there is still some debate if the analysed vascularization is due to angiogenesis or vasculogenesis, since these processes are not completely separated in the developing embryo[64].

8.2.1 The mouse retina assay

The mouse retina assay has been used extensively to study both physiological and pathological angiogenesis. The mouse is the animal model chosen due to the combination of

low cost, available transgenic strains and wide availability of recombinant proteins and antibodies. In addition, at birth, pups present an immature retinal vasculature allowing the study of postnatal retinal development without requiring surgical skills. Moreover, the postnatal retinal vascular development is very organized and tightly regulated, making the retina a reliable model for pharmacological studies[68].

8.2.1.1 Vascular development in the mouse retina

Mice are born without blood vessels in the retina and instead the hyaloid vasculature supplies the retina with oxygen and nutrients. However, around the time of birth, the hyaloid vasculature regresses and a vascular plexus emerges from the optical nerve, which develops into the retinal vasculature[69]. The emerging blood vessels form three separate layers in the retina: the superficial plexus (closest to the lumen of the eye), the intermediate plexus and the deep plexus (Figure 9). The superficial plexus is established during the first week after birth, and reaches the retinal edge approximately around postnatal day 8 (P8). The deep plexus starts developing around P7 when the superficial capillaries sprout vertically and migrate deeper into the retina, reaching rapidly the retina periphery in P12. By P12 the deep plexus reaches the retinal periphery and the last plexus develops in the intermediate layer around P12-P15. All three vascular layers are fully mature by the end of the third postnatal week with vessels that connects the three layers to each other[68]. It is then believed that the superficial plexus is formed by vasculogenesis and the deeper plexus are formed by sprouting angiogenesis[69].

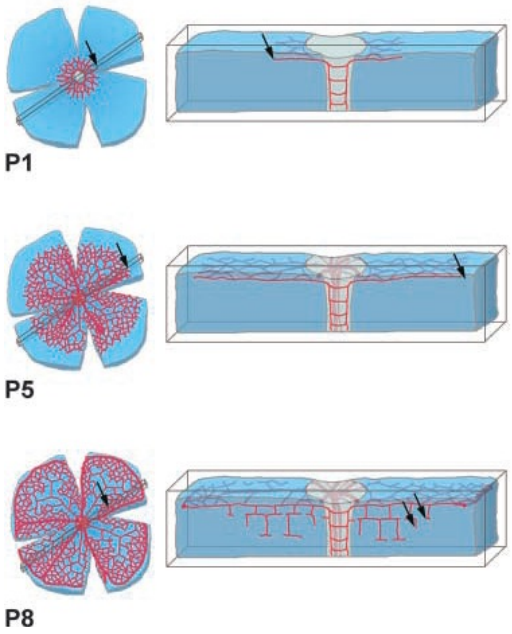

Figure 9: Schematic representation of retinal development. Sprouting occurs toward the periphery in the primary plexus (P1 and P5, arrows), subsequently sprouts into deeper layers (P8)[70]

Chapter II Aims of the Work

The Angiogenesis laboratory, headed by Katerina Tritsaris, has previously shown that IL-27 inhibits proliferation and migration of lymphatic endothelial cells, in part through STAT1-regulated expression of anti-angiogenic chemokines[18]. The molecular mechanisms regulating STAT1 tyrosine phosphorylation are fairly well studied; however, possibly IL-27-induced STAT phosphorylation of serine residues has not been described. Elucidating whether IL-27 induce serine phosphorylation of STAT1 and by which mechanism is important, because serine phosphorylation is essential for full transcriptional activity of STAT1[71].

The central aim of this thesis was to identify new intracellular molecular components responsible for IL-27 signalling in Human Umbilical Vein Endothelial Cells. The hypothesis raised was that IL-27 via activation of MAPKinases phosphorylates STAT1 at serine residues thereby regulating proliferation, survival and migration of endothelial cells. This hypothesis was based on previous studies in the lab and on a paper from Matsumoto and colleagues (2002).

In the end, we want to elucidate IL-27-regulated signalling pathways in order to understand the biological effect of IL-27. The second part of my thesis therefore focuses on selection and optimization of different *in vitro* and *in vivo* angiogenesis assays, with the purpose of defining the optimal assay for measuring reliable effects of IL-27 on angiogenesis. By these experiments I hope to add to the mechanistic understanding of angiogenesis necessary for discovering future drugs for treatment of pathophysiological angiogenesis.

Chapter III Materials and Methods

9 Cells lines and Cell culture

Human Umbilical Vein Endothelial Cell line (HUVEC) was purchased from Lonza (Cat no. CC-2519). This is a primary cell line and can only be used until passage 10, after that the HUVEC lose their ability to divide and experience "phenotypic drift" (when cells double in size). HUVEC were grown in Endothelial Basal media (EBM) supplemented with EGM SingleQuots (which contains Gentamicin, recombinant human Endothelial Growth Factor, Bovine Brain Extract, Ascorbic Acid, Hydrocortisone and Fetal Bovine Serum).

The EA.hy926 cell line was purchased from ATCC (Cat. No. CRL-2922). This is an immortalized cell line, established by fusing primary human umbilical vein cells with a thioguanine-resistant clone of A549 cell line (adenocarcinomic human alveolar basal epithelial cells). EA.hy926 were grown in Dulbecco's Modified Eagle's Medium (DMEM), supplemented with 10% FBS and 1% Penicillin/Streptomycin.

In order to normalize and to obtain comparable experiments using both cell lines, growth conditions were performed in a similar way. Cells were expanded in tissue culture flasks coated with 1% gelatin. Coating was performed by covering the relevant plastic surface with a solution of 1% gelatin in phosphate-buffered saline without $Ca^{2+}/Mg^{2}{}_{+}$ (PBS) followed by an incubation step of at least 30 minutes at 37°C and washing with PBS without Ca^{2+}/Mg^{2+}.

Cells were splitted every two days, when 90-95% confluency was reached and seeded to an estimated confluency of 40-50%. Briefly, medium was removed and cells were washed twice in 1x PBS (without Ca^{2+}/ Mg^{2+}). After PBS removal, 10µL/cm2 of undiluted Trypsin in 0.05% EDTA was added and cells incubated 2-5 minutes in the incubator. The cell suspension was diluted at least 20 times with fresh cell medium and transferred to the relevant flask(s) or dish(es).

Gelatin 1 %: Cat. no. G2500-500g, Sigma-Aldrich
PBS without Ca^{2+}/Mg^{2}+: substrate department at the Panum Institute
Endothelial Basal Media (Lonza, CC-3121)
EGM SingleQuots (Lonza, CC-4133)
DMEM: substrate department at the Panum Institute
Penicillin/Streptomycin, Substrate Department at the Panum Institute
Trypsin in 0.05% EDTA (Lonza, CC-5012)

10 Signal transduction assays

10.1.1.1 Sample preparation

HUVEC were seeded on 1% gelatin-coated tissue culture dishes (6cm) in 4mL cell medium (complete medium) at 50% confluency and allowed to reach about 90% confluency. Cells were washed once in 1x PBS before incubation for 1 hour in 4mL of 2% FBS EBM medium. Stimulation was performed by addition of 20ng/mL rhIL-27.

Inhibition of JNK was achieved by pre-treating HUVEC for 30 minutes with JNK inhibitor II (50µM) before incubation with rhIL-27. JNK inhibitor II is a potent and reversible inhibitor of SAPK/JNK, competing with ATP binding site.

For cellular lysis, medium was aspirated and ice-cold 1x PBS added. After aspiration of 1x PBS, cell lysis was performed by addition of 90µL of Lysis Buffer. The lysates were collected to tubes, spinned down and frozen if not used right way.

Lysis buffer: 4x NuPage Sample Buffer (Cat.no. NP0007, Invitrogen) diluted in deionized H_2O, 1 mg/ml Vanadate, 200mM Sodium Flouride, 1:100 Protease Inhibitor Cocktail (P8340-1ML, Sigma-Aldrich)

10.1.1.2 Gel-electrophoresis

The cell lysates were thawed on ice, mixed by vortexing and then subjected to sonication (2-3 pulses, 60%). Lysates were mixed with 10% (of total volume) of DL-Dithiothreitol (DTT) and heated 10 minutes at 70°C. Equal amounts of protein samples were separated by SDS-PAGE. Electrophoresis chamber was filled with Running Buffer (50mL NUPAGE Running Buffer and 950mL deionized H_2O) and 500µL of Antioxidant was added to the inner chamber. Electrophoresis ran at 200V, 150mA, 25W, for about 1 hour.

DTT, Cat. No. D5545, Sigma-Aldrich
10% Bis–Tris gel, Cat. No. NP0322BOX, Invitrogen
Running Buffer(Cat. no. NP0002, Invitrogen)
Antioxidant (Cat. no. NP0005, Invitrogen)
Magic Marker, Cat. no. LC5602, Invitrogen
Pre-stained ruler, Cat. no. #26616, Thermo Scientific

10.1.1.3 Western blot

Proteins were then transferred from the gel to a nitrocellulose membrane. First, membrane, filter papers and blotting pillows were soaked in 1x Transfer buffer. For correct transfer, sandwich must be prepared and placed in the chamber in following order: cathode, blotting pillow, filter paper, gel, membrane, filter paper, blotting pillow and anode. Transfer

occurred inside a container filled with ice, for 1 hour and 20 minutes, at 98V; 1,02A; 100W. To check correct transfer, membranes were stained with Ponceau diluted 1:5.

Membranes *Filter Paper Sandwich with a 0.45 µm Pore Size* (Cat.no. LC2001, Invitrogen)
1x Transfer buffer was an aqueous solution of 10 % of 10x Blothing Buffer and 20 % of Methanol
10x Blothing Buffer (1 L): 30,3 g Trizma base (Cat. no. T6066-500g, Sigma-Aldrich), 144 g Glycine (Cat. no. , Sigma-Aldrich) dissolved in deionized H_2O (pH should be 8,3 and can't be adjust)
Methanol (Fisher Scientific, cat# A452-4)
Ponceau (cat. no. P7170-1L, Sigma-Aldrich)

Afterwards, membranes were washed shortly with 1x PBS with 0.1% Tween®-20 and were then blocked with 5% Milk protein dissolved in 1x PBS with 0.1% Tween®-20. Membranes were probed overnight at 4°C with antibodies diluted in 1x PBS with 5% Bovine Serum Albumin (BSA), 0.1% of NaN_3 and 0.1% Tween®-20.

Tween® 20 (Cat.no. P1379-500mL, Sigma-Aldrich)
Blotting-Grade Blocker (Cat. no. "170-6404, BioRad)
BSA Cat.no. A8022-50g, Sigma-Aldrich)

Table 1: Primary Antibodies used in Signaling Transduction Assays

Name	Catalog number	Company
c-Jun (L70B11)	#2315	Cell Signaling
GAPDH	#MAB374	Milipore
GBP2 (G-9)	sc-271568	Santa Cruz Biotechnology, Inc.
IRF-1 (D5E4)	#8478	Cell Signaling
p150 [Glued]	610473	BD Biosciences
p38α	AF8691	R&D Systems
p38β2	33-8700	Invitrogen
p38γ	AF1347	R&D Systems
p38δ	AF1519	R&D Systems
Phospho-c-Jun (ser73)	#3270	Cell Signaling
Phospho-p38 (Tyr180/Tyr182)	#9211	Cell Signaling
Phospho-STAT1 (Ser727)	#9177	Cell Signaling
Phospho-STAT3 (Ser727)	#9134	Cell Signaling
Phospho-STAT5 (Tyr694)	#9351	Cell Signaling
STAT1	#9172	Cell Signaling
STAT3 (124H6)	#9139	Cell Signaling
STAT5 (3H7)	#9358	Cell Signaling

Subsequently, membranes were incubated for 1 hour in 1x PBS with 1% Milk protein and 0.1% Tween®-20 with peroxidase conjugated goat anti-rabbit Immunoglobulin antibody or with peroxidase-conjugated goat antimouse immunoglobulin antibody diluted 1:1000. Protein bands were detected using supersignal West Pico or Femto chemiluminescent substrate and visualized using the biospectrum AC imaging system (UVP, Cambridge, UK).

peroxidase conjugated goat anti-rabbit immunoglobulin antibody Cat.no. P0448, Dako
peroxidase-conjugated goat anti-mouse immunoglobulin antibody Cat.no. P0447, Dako
supersignal west pico chemiluminescent substrate Cat.no. #34080, ThermoScientic
supersignal west femto chemiluminescent substrate Cat.no. #34096, ThermoScientic

All images were quantified using UN Scan it gel software, followed by statistical analyses by GraphPad Prism 5, using a One-way ANOVA test and post-test Dunnett or Bonferroni. All the data are represented as mean ± standard deviation (SD).

11 RNA purification:

HUVEC were seeded on 1% gelatin-coated tissue culture dishes (10cm) in 8mL cell medium (complete medium) at 50% confluency and allowed to reach about 90% confluency. Cells were washed once in 1x PBS before incubation for 1 hour in 8mL of 2% FBS cell medium. Stimulation was performed by addition of at 20ng/mL rhIL-27.

Total RNA was extracted from HUVEC using the RNeasy® mini kit according to the manufacturer's instructions. Briefly, cells were disrupted for 15min in RTL buffer with β-mercaptoethanol and the lysate was pipetted to a QIAshredder spin column and centrifuged for 2 minutes at full speed. One volume of 70% ethanol was added to the homogenized lysates. Samples were transferred to RNeasy spin columns and centrifuged. DNase digestion step was performed by addition of a mix of 10µL of DNase I stock solution with 70µL RDD buffer to the column, followed by 15 minutes incubation. Successive washes were performed and RNAse-free water was added to elute RNA.

RNA purity and concentration was determined measuring 260nm/280nm and 260nm/230nm ratios using a NanoDrop® ND-1000 spectrophotometer. A 260nm/280nm ratio above 2 and a 260nm/230nm ratio above 1.7 were considered to indicate RNA of sufficiently high purity for reverse transcription. Until usage, samples were kept at -80°C.

RNeasy® mini kit: cat. no.: 74104, Qiagen

11.1 Reverse transcription and Real Time-Polimerase Chain Reaction (Q-PCR)

Real time-PCR was performed to quantify mRNA levels in HUVEC treated for different time intervals with rhIL-27 (20ng/mL). Real-time PCR consists of two steps: Reverse Transcription, to synthesize cDNA from RNA samples and Q-PCR, where cDNA is quantified.

11.1.1.1 Reverse transcription:

- Omniscript® RT kit

  0.25µg of template RNA was mixed with 2µL of each 10x RT buffer, 5mM dNTP mix and of 10mM Oligo-dT primer, 1µL of each 10U/µL RNase inhibitor and Omniscript Reverse Transcriptase. RNase-free H_2O was added until total volume of 20µL.

  Reactions tubes were placed in a thermal cycler at 37°C for 60 minutes. In the end, cDNA is diluted 1:1 in RNase-free H_2O and stored at 4°C or -20°C for long storage.

- Phusion RT-PCR kit

  0.25µg of template RNA was mixed with 1µL of each 10mM dNTP mix and Oligo(dT) primer. RNase-free H_2O was added until total volume of 10µL. To pre-denature RNA mix was incubated for 5 minutes at 65°C and immediately placed on ice. To each tube was added 2µL of each 10x RT buffer and RT enzyme mix. 6µL of RNase-free H_2O were also added and reaction tubes were placed in thermal cycler with following program.

Table 2: Thermal cycler set up for Reverse Transcription using Phusion RT-PCR kit

Step	Temperature	Time
Primer Extension	25 °C	10 min
cDNA synthesis	40 °C	30 min
Reaction termination	85 °C	5 min
Cooling	4 °C	hold

In the end, cDNA is diluted 1:1 in RNase-free H2O and stored at 4°C or -20°C for long storage.

Omniscript® RT kit: cat. no.: 205111, Qiagen
Phusion RT-PCR kit: cat. no.: F-546S, Finnzymes

11.1.1.2 Q-PCR

Real-time PCR was performed based on the protocol for Light Cycler® 480 SYBR Green I Master. Briefly, in each reaction tube was added 10µL of 2x concentrated Master Mix (contains FastStart Taq DNA Polymerase, reaction buffer, dNTP mix (with dUTP instead of dTTP), SYBR Green I dye and $MgCl_2$), 0.3µL of 2µM ROX and 2µL of cDNA. Volume of primers was added according to the concentration required and RNase-free H_2O was added until a total volume of 20µL.

The 96 well-plate was centrifuge to prevent bubbles in reaction tubes and PCR was performed in a MX-3000P thermal cycler from Stratagene with the following set up.

Table 3: Thermal cycler set up for Q-PCR

Step	Temperature	Time	Cycles
Pre- Incubation	95 °C	10 min	1
Amplification	95 °C	20 sec	45
	Primer dependent	22 sec	
	72 °C	20 sec	
Melting Curve	95 °C	1 min	1
	55 °C	30 sec	
	95 °C	30 sec	

Light Cycler® 480 SYBR Green I Master: Cat.no.: 04 887 352 001, Roche

11.1.1.3 Optimization steps

For an accurate result it is required to optimize both the reverse transcription and the real time-PCR.

First, in Reverse Transcription, it is necessary to inactivate Reverse Transcriptase (RT) after the reverse transcription reaction, as this enzyme might influence in the amplification step of Q-PCR[72]. For this reason I tested two different reverse transcriptase kits: Omniscript® RT kit from Qiagen and Phusion RT-PCR kit from Finnzymes.

In Real Time-PCR step there are several determinant steps to take attention. Starting with the primer design, all primers were designed with National Center for Biotechnology Information (NCBI) Primer-Blast tool with the Refseq mRNA database (organism limited to Homo sapiens). When designing them, we were careful to be certain the product size ranged between 70 – 300 base pairs. Annealing temperature was set as optimal for 60°C with a deviation of 2°C. Only 1°C allowed as difference in annealing temperature between forward and reverse primers. It is also very important to design primers that target a sequence with an internal intron, by this it is possible to verify the product size and assure that the amplification arise from cDNA and not gDNA that might exist in the sample

We wanted to test p38α mRNA level and because of that we ordered 4 different sets of primers (Primers sequence in Appendix 1). In order to optimize the best pair of primers, a Real-Time PCR, using 150mM of each primer and an annealing temperature of 60°C was performed. The best primer pair was chosen based on the Dissociation curve; this should occur as a single peak, representing amplification of only one product. Additionally a low cycle threshold (Ct) value was taken into account.

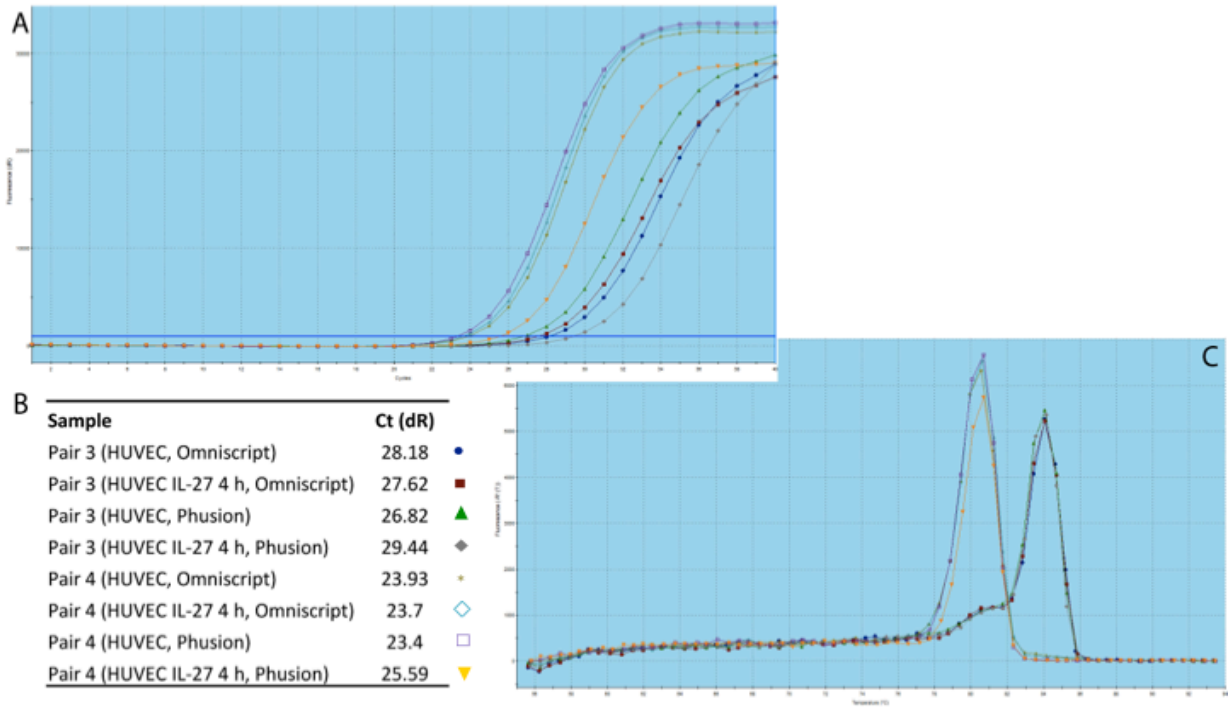

Figure 10: Test of Primers pairs 3 and 4, at 150mM and annealing temperature of 60°C. It was tested two conditions (HUVEC left unstimulated and HUVEC stimulated with IL-27 for 4 hours). Also cDNA was synthesized using two Reverse Transcription kits: Omniscript® RT and Phusion RT-PCR A: Amplification Curve; B: Ct values for each sample, corresponding to Amplification Curves; C: Dissociation Curves, peaks at lower temperature corresponds to primer pair 4 and peak with small shoulder at higher temperature corresponds to primer pair 3. Each sample was analyzed in triplicate, values shown are the mean.

The first two primer pairs were eliminated through observation of Dissociation curve (Appendix 1). Figure 8 shows test of two primer sets using cDNA from reverse transcription of RNA using either Omniscript or Phusion RT kits. RNA was original from cells either unstimulated or stimulated with IL-27 for 4 hours.

Through observation of Dissociation Curve for primer pairs 3 and 4, it is possible to eliminate pair 3, since this shows a “shoulder”. This can mean two things: primers are not specific for the target sequence, so the value of amplification observed is not accurate, or there is primer dimer, once again, preventing us to observe real amplification of the target sequence. Also, Ct values of pair 3 are much higher than Ct for pair 4.

Primer pair 4 was selected since it showed a clean Dissociation curve with a single peak. In addition, Ct values presented were lower than Ct for pair 3. It was also decided to proceed with cDNA from Phusion RT kit because this showed a lower Ct for the unstimulated sample, comparing with the Omniscript RT kit.

After choosing the primers to be further used and to obtain the best reaction possible it was tested different combinations of concentrations for both forward and reverse primers (Table 4).

Table 4: Primer pair 1 for p38α concentrations and combinations tested.

Forward	Reverse	Sample	Forward	Reverse	Sample
50 nM	50 nM	1	300 nM	50 nM	9
	150 nM	2		150 nM	10
	300 nM	3		300 nM	11
	600 nM	4		600 nM	12
150 nM	50 nM	5	600 nM	50 nM	13
	150 nM	6		150 nM	14
	300 nM	7		300 nM	15
	600 nM	8		600 nM	16

The best primer concentration is chosen, not only due to Ct value, but also owing to the maximum fluorescence obtained.

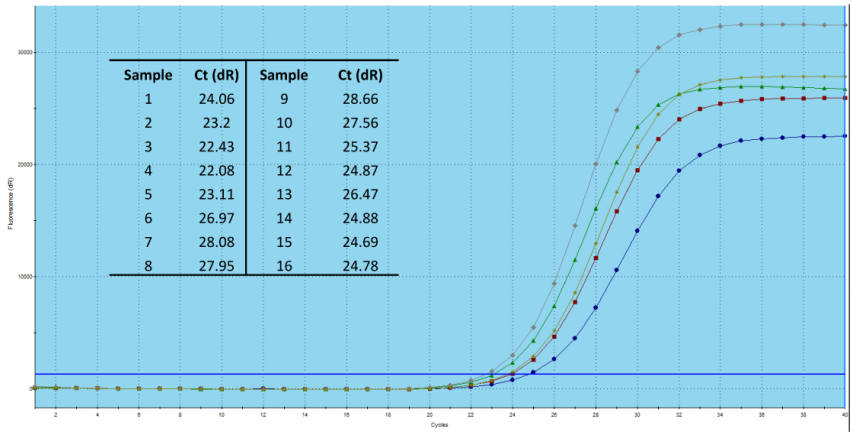

Figure 11: Test of different concentrations of primer pair 4. Amplifications curves of first 5 samples (from lower Ct to higher with the following order: 4, 3, 5, 2, 1). Table with Ct values for all samples tested. Each sample was analyzed in triplicate, values shown are the mean.

A lower Ct and a higher fluorescence was obtained in sample 4 (Forward: 50mM and Reverse: 600mM, in Amplification graph: grey line, Figure 11) compared to the other combinations. Yet this condition was not selected because 600mM is an excessively high concentration, which can result in primer dimer formation at low target concentrations. An optimal concentration to work with should be near to 150mM, for that reason, study was followed with concentrations from sample 5 (Forward: 150mM and Reverse: 50mM, yellow line in Amplification graph, Figure 11), which still presents a low Ct.

Next step, required for future quantification, was to perform a Standard Curve, for primers used in the study including a housekeeping gene. In order to make a standard curve we began by diluting the cDNA to be used 1:4, eight consecutive times. Q-PCR mixture was then prepared in the same way as previously described.

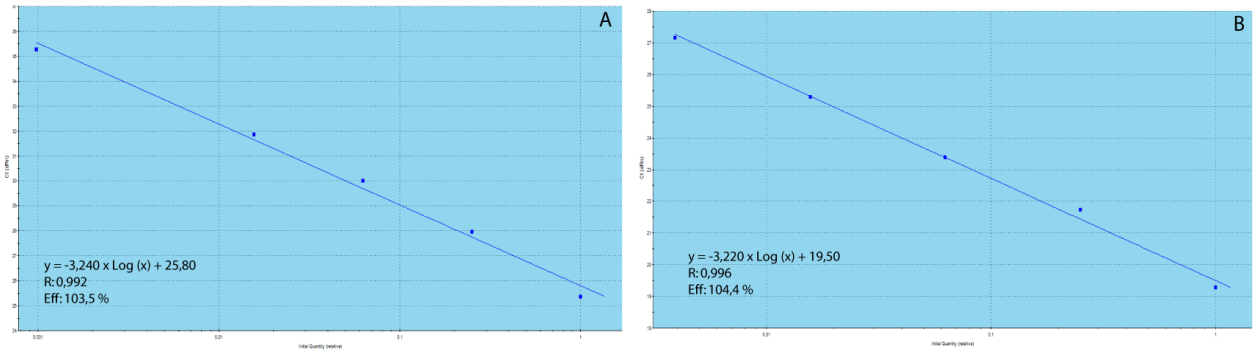

Figure 12: Standard Curves for p38α primer pair 4 (A) and GAPDH (B). Each sample was analyzed in triplicate, values shown are the mean.

With an accurate standard curve is possible to analyze the quantity of p38α mRNA in different samples. Calculations were performed using the *Pfaffl* Method[73]. Basically, the general equation is:

$$ratio = \frac{(Eff_{target})^{\Delta Ct\ target\ (Control-treated)}}{(Eff_{ref})^{\Delta Ct\ ref\ (Control-treated)}},$$

Eff is efficiency obtained in Standard curve; target is the gene in study, in this case p38α and reference is GAPDH.

As part of optimization steps, it is also important to adjust the annealing temperature for each primer set, preventing for instance primer dimer in the reaction. We did not perform this step because primer pair 4 already showed a high degree of accuracy.

12 Immunofluorescence

HUVEC were seeded on gelatin-coated coverslips in culture dishes (4cm) in 3mL cell medium (complete medium) at 50% confluency and allowed to reach about 90% confluency before starting the experiment.

The cell medium was aspirated and cells were washed once in PBS before incubation for 1 hour in 2% FBS EBM medium. After incubation, cells were stimulated with rhIL-27 (20ng/mL), in the same medium as during the incubation, at the desired time points.

Cells were washed once in 1x PBS and fixed for 30 min in 4% Paraformaldehyde (PFA, 1.5mL/dish). After three successive washes with 1x PBS, coverslips were stored at 4°C in 1x PBS till usage.

Coverslips were covered with ice-cold 100% methanol for 10 minutes at -20°C to permeabilize cells. Next, they were incubated with Blocking Buffer (5% NGS (Normal Goat

Serum), 0.3% Triton X-100, 1x PBS) for 2 hours. Incubation with primary antibody, diluted in 1% FBS, 0.3% Triton X-100, 1x PBS, was performed overnight at 4°C.

The following day, coverslips were incubated with secondary antibody, diluted in 1% FBS, 0.3% Triton X-100, 1x PBS, for 2 hours in the dark. Coverslip slides were mounted with VectaField fluorescent mounting media (with DAPI) and stored at 4°C, while avoiding direct light, until observation in Fluorescence Microscope. Images were manipulated with MetaMorph software.

Methanol (Fisher Scientific, cat# A452-4)
32 % Paraformaldehyde Cat.no. #15714-S, Electron Microscopy Sciences
Triton X-100 Cat.no. X100-100mL, Sigma-Aldrich
VectaField fluorescent mounting media Cat.no.H-1200, Vector Laboratories Inc.
Superfrost Plus Microscope Slides (Fisher Scientific, Cat# 12-550-15)

Table 5: Primary antibodies used in Immunofluorescence.

Primary Antibody	Dilution	Company
IRF-1	1:200	Cell Signaling
P-SAPK/JNK (Thr183/Tyr185)	1:400	Cell signaling
P-STAT5 (Tyr694)	1:100	Cell Signaling
GBP2	1:50	Santa Cruz Biotechonology

Secondary Antibodies used in Immunofluorescence
Anti-rabbit IgG F(ab')$_2$ (AlexaFluor®488 Conjugated), 1:1000 dilution. Cat.no #4412, Cell Signaling
Anti-mouse IgG F(ab')$_2$ (AlexaFluor®555 Conjugated), 1:1000 dilution. Cat.no #4409, Cell Signaling

13 Proliferation Assay

Method was performed using the BrdU Cell Proliferation Assay kit from Calbiochem according to manufactures instructions. This is a colorimetric assay, which functions by incorporation of Bromodeoxyuridine (a thymidine analog) in DNA of proliferating cells.

Briefly, 200µL of HUVEC (2 x 10^3 cells) were seeded in 96-well plate coated with 1% gelatin. Next day fresh medium (with rhIL-27 or FGF or combination of both) was added and cells were incubated for 24 hours. 20µL of BrdU diluted in 1x PBS was added to all wells (except to the Background control). After 6 hours cells were fixated for 30 min, incubated with Anti-BrdU antibody for 1 hour, followed by incubation with Peroxidase Goat Anti-mouse for 30 minutes. The plate was washed carefully to ensure there was no residue left and was then incubated 15 minutes, in the dark with Substrate solution. Reaction was stop with Stop solution and absorbance was measured within 15 minutes in a *Synergy HT* microplate reader from BioTek, at dual wavelengths of 450-540 nm.

Cat. No. QIA58, Calbiochem (Merck, Germany)

14 Endothelial cells Spheroid-based Angiogenesis Assay

This assay was performed based on the method described by Korff and Augustin (1999). Spheroids were generated by seeding 500cells/100µL in each well of a 96-well non-adherent round-bottom plate, in complete medium containing approximately 0.26% of Methylcellulose. Incubation was for 18 hours, at 37°C and 5% CO_2, which resulted in a single spheroid per well. rhIL-27, in different concentrations, was added to each well and spheroids were incubated for 6 hours in the same conditions as before.

Collagen gel was prepared by mixing rat-tail Collagen I with 10% (volume) of 10x DMEM and 1M NaOH to adjust pH to approximately 7.4. Thereafter it was mixed in a ratio 1:1 with complete medium containing 20% FBS and 1.3% Methylcellulose. In a 24-well plate, a 200µL layer of Collagen-Methylcellulose mixture was added and let to polymerize for a few minutes. Spheroids were collected from the 96-well non-adherent round-bottom plate, centrifuged at low rotation, carefully mixed with 600µL of the Collagen-Methylcellulose mixture and plated on the top of each layer. The same number of spheroids was plated in each well. After of 30 minutes of incubation at 37°C and 5% CO_2, 200µL of complete medium was added and stimulated with or without rhIL-27 for 24 hours.

Spheroid sprouting was imaged using a Leitz Labovert phase-contrast microscope (Leyca Microssystems) and a CoolPix 990 digital camera (Nikon). Pictures manipulation was performed using ImageJ software.

Methylcellulose: (Sigma-Aldrich, cat. no.: 274429-500G)
rat-tail Collagen I, ≈ 4 mg/ml (BD-Biosciences, cat. no.: 354236)
10x DMEM (Sigma-Aldrich, cat. no.: D2429)
1M NaOH

14.1.1.1 Critical steps

First, to create each spheroid was necessary to seed cells in a mix of medium with about 0.26% of Methylcellulose, this is a viscous mixture that allows the cells to maintain in suspension. To prepare this mix we need to centrifuge it for 2 hours at 5000xg, after what is possible to observe two phases. All impurities stay in the bottom part, looking like a cloudy solution, but without a clear separation. If we have impurities in this mix, spheroids will not assemble correctly. It is also important to be certain of the number of cells and to mix it always before seeding the cells in order to prevent cells falling in the bottom of the tube. In

addition, while seeding the cells we should not create bubbles, as this appears to affect spheroid assemble.

Next critical step is taking spheroids from the Methylcellulose and incorporating them in the collagen matrix. Carefully we need to remove the spheroids, for this reason is necessary to always cut the tip of the pipet used to remove the spheroids. These are then centrifuge at low rotation, only to be certain they stay in the bottom. Again, all this steps to prevent the cells to detach from each other's.

We also included in the protocol a thin layer in each well only with collagen matrix, this will allow the spheroids to grow in a 3D fashion. It was observed before by this laboratory that sometimes spheroids fall in the bottom, starting to spread as in a 2D culture, if we allow this layer to polymerize for about 5 minutes, incorporation of spheroids is still possible.

Finally, as in the first step, cannot exist bubbles in the matrix, as this was seen to affect the sprouting. Also it is important to keep humidity stable, so in surrounding wells should be added 1x PBS.

15 Endothelial Cell Tube Formation Assay

This method was performed based on the protocol provided by BD Biosciences. In order to pre-stimulate cells, HUVEC were seeded on gelatin-coated tissue culture dishes (6cm) in 4mL of 2% cell medium at 50% confluency and allowed to attach for a few hours. Dishes were then pre-stimulated with different concentrations of rhIL-27. One dish was stimulated with FGF as a positive control for proliferation. Incubation was performed for at least 12 hours.

Growth Factor Reduced (GFR) Matrigel was thawed overnight on ice at 4°C. Also the necessary plates and tips were kept at 4°C overnight. Using cooled pipets, Matrigel was homogenized and added to each well (290µL for a 24 well-plate; 50µL for a 96 well-plate). The plate was then incubated at 37°C for about 1 hour. Cells from each condition were trypsinized, centrifuged and re-suspended in 2mL of 2% FBS medium. Cells were counted and diluted to a concentration of $4x10^5$ cells/mL (24 well-plate) or between 0.5-1.5 x 10^4 cells/mL (96 well-plate). In each well the cell suspension was added with the respective stimulator (300µL in 24 well-plate; 100µL in 96 well-plate). All conditions were seeded in duplicate Plates were incubated at 37°C, 5% CO_2 and followed for 24 hours.

Tube Formation was imaged using a Leitz Labovert phase-contrast microscope (Leyca Microssystems) and a CoolPix 990 digital camera (Nikon).

Growth Factor Reduced (GFR) Matrigel: Cat.no.: 356231, BD Biosciences

16 *In vivo* mice Retina Angiogenesis

Mice were sacrificed by cervical dislocation. Eyes were removed and placed in 4% PFA for 5 minutes, after that the eyes were transferred to 2% PFA. Retina dissection was performed in the microscope, in a petri dish lid filled with PBS. Briefly, cornea was dissected to allow the lens to be removed. Sclera was grasped and carefully detached from the retina using forceps. Retinas underwent radial cuts and were transferred back into clean 2% PFA. Retinas were left in this condition overnight at 4°C. Ice cold 100% Methanol was added to permeabilize the retinas for 10 minutes. After a washing step, retinas were blocked using 20% FBS, 20% NGS and 0.2% Triton X-100 in PBS, at room temperature for 2 hours before incubation with Isolectin-GS4 diluted 1:200 in PBS with 10% NGS and 10% FBS at room temperature, on an orbital shaker and in the dark, for 2.5 hours. Still on an orbital shaker, set for low speed and in the dark, 1x PBS was added and incubated for 1.5 hours. PBS was replaced every 20-30 minutes. To post fix retinas these were incubated 10 minutes with 2% PFA. Retinas were mounted on Microscope slides and visualized by use of Confocal Microscope.

Isolectin GS-IB4, Alexa Fluor-647 conjugate (Invitrogen, Cat# I32450)
(Isolectin B4 is a tetrameric glycoprotein, isolated from the Griffonia Simplicifolia seeds, that binds exclusively to D-galactose and is used to label endothelial cells in mouse tissues 72.)

17 Cytokines

Cytokines were handled according to the manufacturer's specifications.

Recombinant human IL-27: Cat.no. 2526-IL-010 , R&D Systems
FGF-2, Sigma-Aldrich (prod.no.: SRP4037)
Recombinant mouse IL-27, R&D Systems (prod.no.: 2799-ML/CF)

Chapter IV Results

IL-27 induces serine^{727} phosphorylation of STAT1

It has previously been shown that IL-27 has anti-angiogenic effect on vascular endothelial cells[10] as well as anti-proliferative effect on lymphatic endothelial cells via STAT1[17]. However, the mechanism by which IL-27 regulates STAT1 activity is not fully understood. In order to get wider insights into IL-27-regulated signalling I investigated potential serine phosphorylation of STAT1.

To determine the serine phosphorylation patterns of STAT1 and STAT3 induced by IL-27 in HUVEC, cells were stimulated with IL-27 (20ng/mL) for an 8 hours time-course and serine phosphorylation visualized by immunoblotting.

Western blot analysis revealed that STAT1 phosphorylation on serine^{727} occurred after 15 minutes in the presence of IL-27 and gradually increased until 2 hours. No decrease in phosphorylation was observed from 2-8 hours (Figure 13A). Membranes were quantified, revealing a significant increase in STAT1 serine^{727} phosphorylation after 45 minutes of stimulation, compared to unstimulated (Figure 13B).

Phosphorylation of serine^{727} on STAT3 did not alter throughout the time period, thus this protein is not serine phosphorylated in response to IL-27 in endothelial cells.

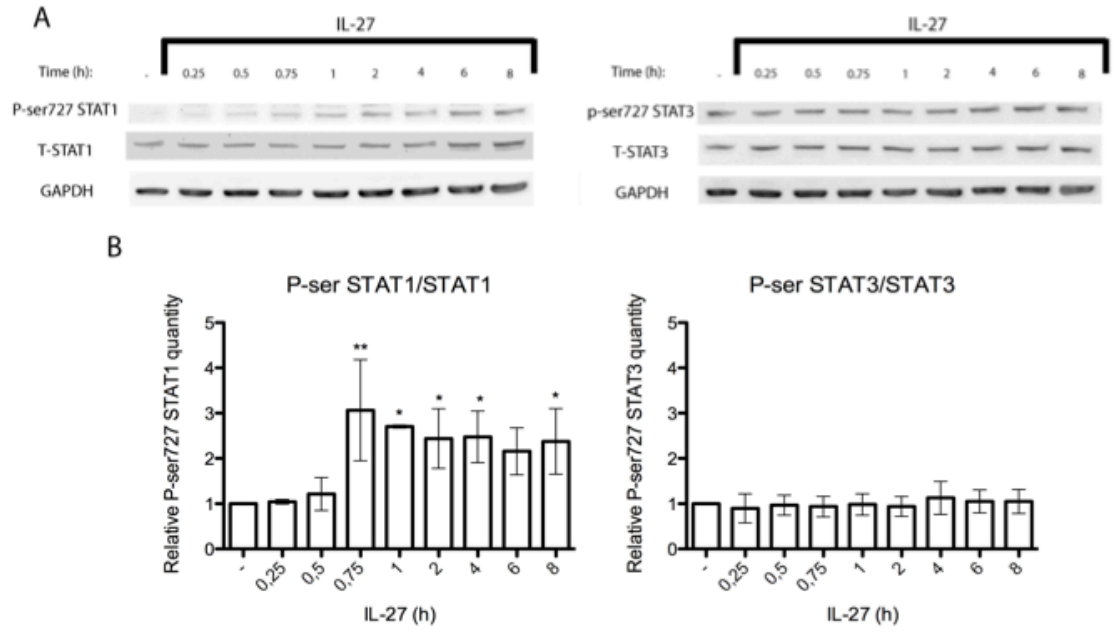

Figure 13: STAT1 serine 727 is phosphorylated following IL-27 stimulation of HUVEC. HUVEC were stimulated with IL-27 (20ng/mL) and lysed by addition of cell lysis buffer at the indicated times. A: Cellular lysates were used for immunoblotting with antibodies against STAT1 phosphorylated at serine727, STAT3 phosphorylated at serine727, Total STAT1 and Total STAT3. GAPDH was used as control. Data are representative of three independent experiments. B: Graphical representation of Western Blot quantification. Mean of three experiments with respective Standard deviation. Samples were compared to control using Dunnett's post test; **: $p < 0.001$; *: $p < 0.05$.

IRF-1 activation is dependent on STAT1 after IL-27 stimulation

According to the literature, IRF-1 is expressed downstream as a consequence of IFNγ-induced STAT1 serine phosphorylation[74]. IRF-1, a tumor suppressor and transcriptional modulator, has been shown to have an anti-angiogenic effect in endothelial cells[75] and thus might be a useful target for treatment of cancer and angiogenesis-associated diseases.

In order to elucidate whether IL-27 could activate IRF-1 expression Western Blotting using antibody against Total IRF-1 was performed. As it is easily observed there is higher expression of IRF-1 from 2-8 hours in the presence of IL-27 (Figure 14A).

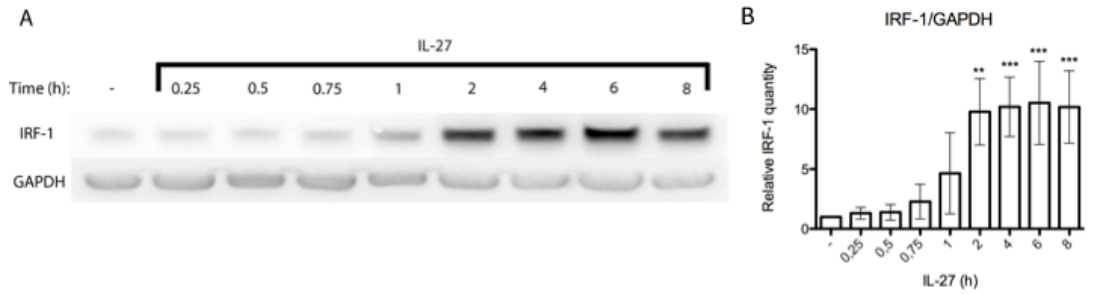

Figure 14: IRF-1 is expressed following IL-27 stimulation of HUVEC cells. HUVEC were stimulated with IL-27 (20ng/mL) and lysed by addition of cell lysis buffer at indicated times. A: Cellular lysate was used for immunoblotting with antibody against Total IRF-1. GAPDH was used as loading control. Data are representative of three independent experiments B: Graphical representation of Western Blot quantification. Mean of three experiments with respective Standard deviation. Samples were compared to control using Dunnett's post test; ***: $p < 0.0001$; **: $p < 0.001$

In order to determine whether IRF-1 expression was dependent on STAT1 activity a STAT1 knockdown experiment was performed by a colleague from the laboratory (Sebastian Rune Nielsen). Cells were incubated for 6 hours with 50nM of STAT1 siRNA or scrambled siRNA, followed by incubation in complete cell medium for 2 days. Cells were then stimulated with 20ng/mL IL-27 for 6 hours and cells lysates were used for immunoblotting (Figure 15).

Figure 15 clearly shows efficient knockdown of STAT1 protein. When the membranes were incubated with Total IRF-1 antibody it became evident that the reduction in STAT1 protein leads to reduce IRF-1 expression. Thus, IRF-1 expression is dependent on STAT1 activity.

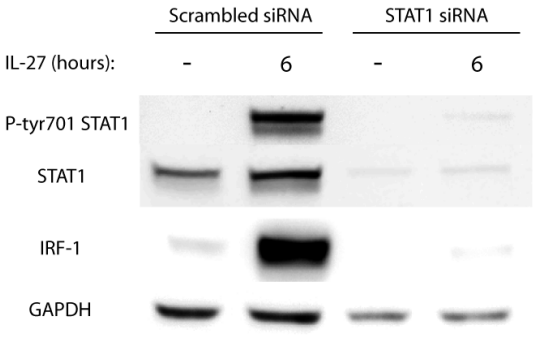

Figure 15: IRF-1 expression decreases after STAT1 knockdown. STAT1 knockdown in the EA.hy926 cell line, using STAT1 siRNA and Scrambled siRNA as control. Cells were stimulated with IL-27 (20ng/mL) for 6 hours and lysed by addition of cell lysis buffer. Cellular lysates were used for immunoblotting with antibodies against phosphorylated STAT1 (Tyr701), Total STAT1 and Total IRF-1. GAPDH was used as loading control.

Canonical STAT signalling leads to translocation of STATs to the nucleus and concomitant transcription of STAT target genes[33,35,36]. Our laboratory has shown that STAT1 phosphorylated at tyrosine[701] is present in the nucleus after IL-27 stimulation (data not shown). We still do not know if serine phosphorylation influences in STAT1 localization or if it is a pre-requisite for STAT1 translocation. Additionally, it is known that IRF-1 is constitutively localized in the nucleus[57]. After revealing that IL-27 activates IRF-1 expression via STAT1, we wanted to determine if IL-27 influences IRF-1 localization since this could give us insight into the function of IRF-1.

Immunofluorescence revealed that IRF-1 was localized in the nucleus, at all time-points, although some diffuse staining in the cytoplasm can be observed at early time-points (Figure 16). From 30 minutes, an increase in IRF-1 can be seen and at 2 and 4 hours IRF-1 exists exclusively in the nucleus.

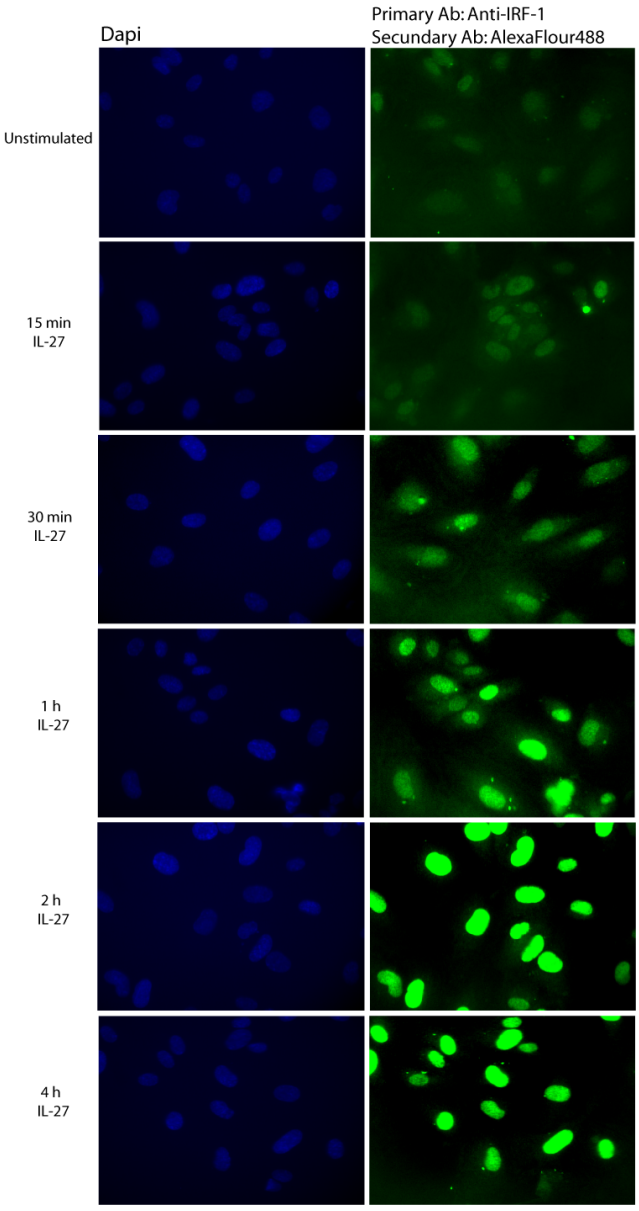

Figure 16: IRF-1 is localized in the nucleus after stimulation with IL-27. HUVEC stimulated for different time periods with 20ng/mL of IL-27. Cells were stained with total IRF-1 antibody and AlexaFlour488 (green). In addition nuclei were stained with DAPI (blue). Images are representative of two independent experiments.

p38 is not responsible for STAT1 serine^{727} phosphorylation

Previous research clearly relates p38 with STAT1 serine phosphorylation in situations of stress or inflammation[37]. In addition, previous experiments performed in the lab showed evidence of p38 phosphorylation upon IL-27 stimulation (data not shown).

To address if p38 is responsible for STAT1 serine phosphorylation after IL-27 stimulation, an 8 hours time-course was performed and the cell lysates used for immunoblotting. Membranes were incubated with all antibodies targeting each p38 isoform (p38α, β, γ and δ) in order to test for IL-27-induced p38 expression and antibodies specific for Threonine^{180} and Tyrosine^{182} phosphorylated p38 to test for p38 phosphorylation.

There seems to be a tendency towards a higher level of p38α in cells stimulated with IL-27 (Figure16, lane1); however, is not possible to conclude, because the loading control (GAPDH) reveals variations in the protein level between samples (Figure 17).

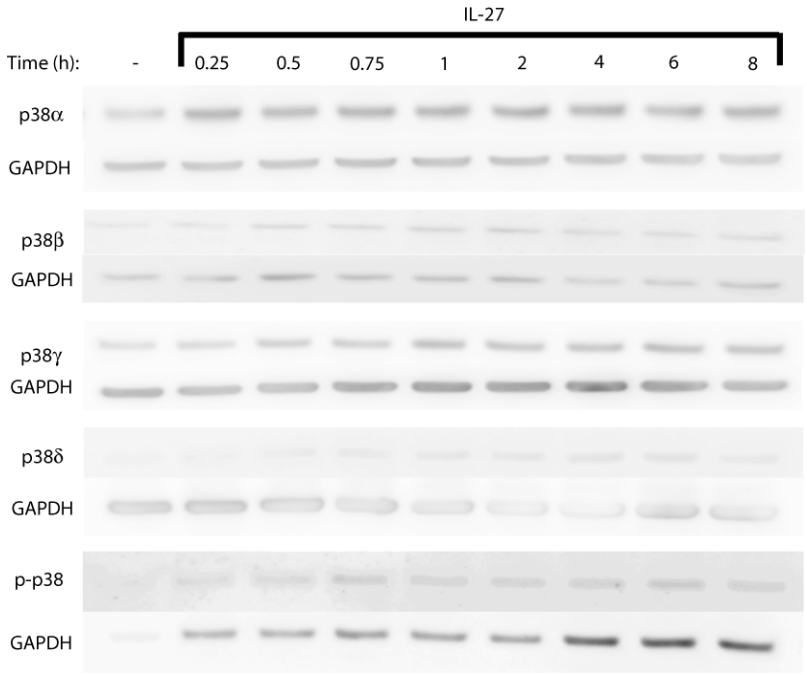

Figure 17: p38α expression in HUVEC cells stimulated with IL-27HUVEC were treated with IL-27 (20ng/mL) and cells were lyzed at the time points shown. Cellular lysates were then immunoblotted with antibodies against p38α, p38β, p38γ, p38δ and phosphorylated p38. GAPDH was used as loading control. Data are representative of two independent experiments.

Since the western results indicated IL-27 stimulated p38α expression we decided to look for p38α expression at the mRNA level.

After optimizing the primers for Q-PCR (as described in the methods section) I measured the level of p38α mRNA at two different conditions: HUVEC unstimulated and HUVEC

stimulated for 4 h with IL-27. Q-PCR was performed with p38α primers and primers for GAPDH as reference.

The Amplification curve showed no difference in the Ct for GAPDH. This was expected because GAPDH is a reference gene, and its expression should be constant. Unfortunately, there was no clear difference in the Ct values for p38α expression between samples treated with IL-27 and control either. This became evident after using the *Pfaffl* Method[73] to calculate the fold change. Only a diminutive (non-significant) decrease in the p38α mRNA level was determined (Figure 18). For this reason it was decided not to continue searching for p38 expression upon IL-27 stimulation.

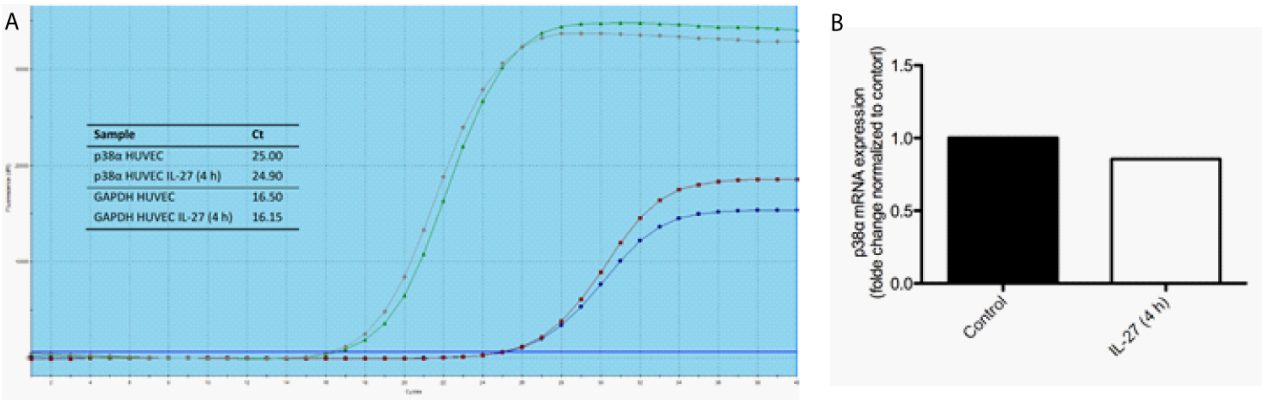

Figure 18: Effect of IL-27 stimulation on p38α mRNA levels . Q-PCR with cDNA from HUVEC stimulated 4 hours with IL-27 (20 ng/mL). Primers were designed to amplify p38α and GAPDH. A: Amplification curves with respective Ct values. B: Graphical representation of quantification through *Pfaffl* Method.

Since IL-27 neither induced expression nor phosphorylation of P38 it did not appear to be the MAPK responsible for STAT1 serine[727] phosphorylation upon IL-27 stimulation. I therefore decided to analyse if the SAPK/JNK was participating in this pathway.

SAPK/JNK is phosphorylated after IL-27 stimulation

I started by analysing the phosphorylated SAPK/JNK present in cell lysates when stimulated with IL-27 for different time-periods because phosphorylation at Thr183/Tyr185 indicates the kinase is active. The cell lysates where used for immunoblotting and membranes were incubated with an antibody against SAPK/JNK phosphorylated at Threonine[183] and Tyrosine[185]. This antibody recognizes two SAPK/JNK isoforms, p46 and p54.

The results indicate that after 30 minutes of IL-27 stimulation there was an increase in phosphorylation of the p46 isoform of SAPK/JNK, which reached a maximum after 4 hours of stimulation with IL-27. However phosphorylation of the p54 isoform reached a maximum after 2 hours of stimulation with IL-27 (Figure 19A). Both isoforms show dephosphorylation at 6 and 8 hours with IL-27.

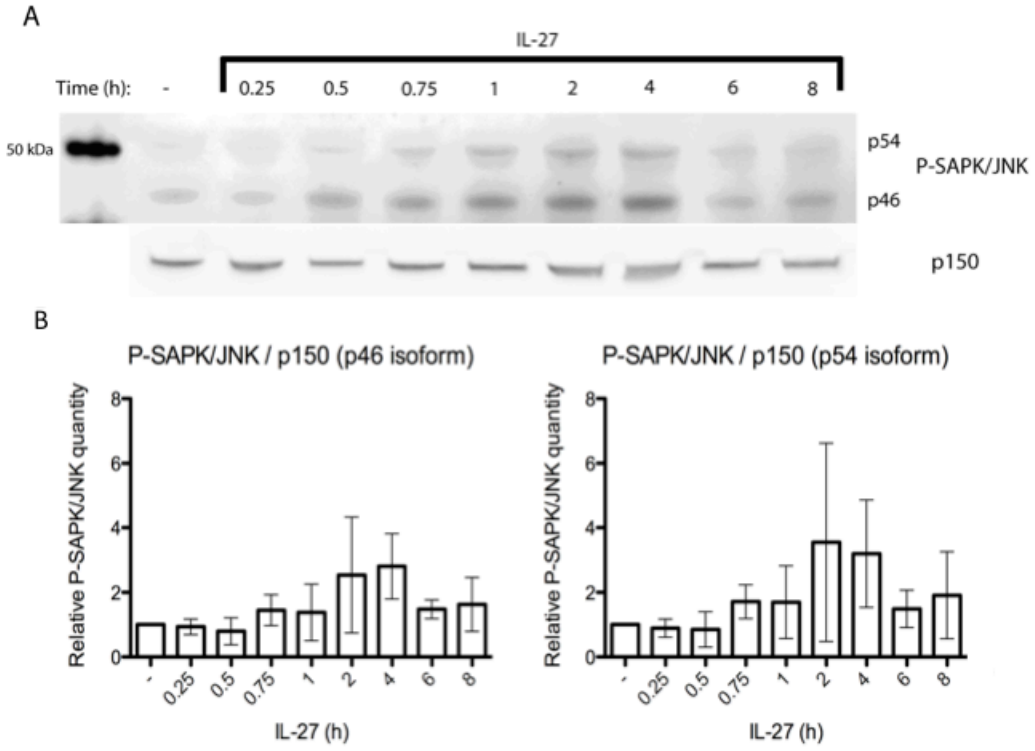

Figure 19: IL-27 stimulates both SAPK/JNK isoforms. HUVEC were stimulated with IL-27 (20ng/mL) and lysed by addition of cell lysis buffer at the indicated time points. A: Cellular lysates were used for immunoblotting with antibodies against phosphorylated SAPK/JNK and p150 (loading control). Data are representative of three independent experiments. B: Graphical representation of Western Blot quantification. Mean of three experiments with respective Standard deviation.

Localization of phosphorylated SAPK/JNK in cells stimulated 2, 6, and 24 hours with IL-27 was then addressed through immunofluorescence. At all time-points a granny staining of phosphorylated SAPK/JNK was visualized (Figure 20), indicating a vesicular localization. It was not possible to observe a difference in fluorescence intensity; however, nuclear localization can be observed after 24 hours.

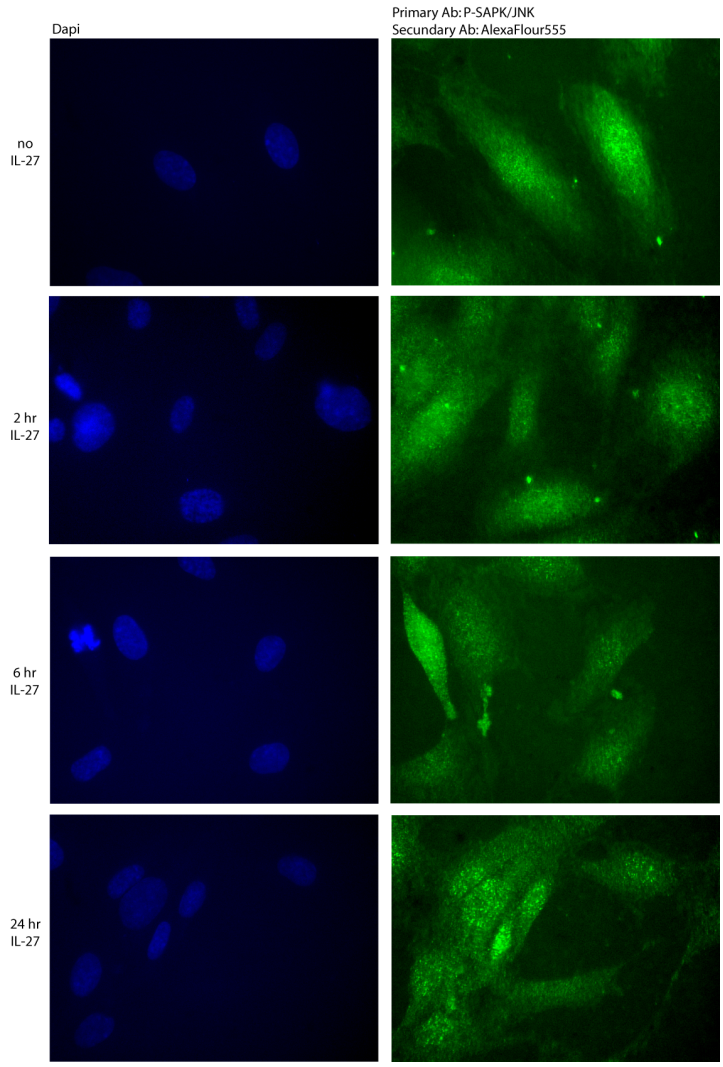

Figure 20: Phosphorylated SAPK/JNK is localized in organelles membrane. HUVEC incubated for different time points with 20ng/mL of IL-27. Incubation with antibody against phosphorylated SAPK/JNK followed by incubation with AlexaFlour555 (green) and DAPI (blue). Images are representative of two independent experiments

Inhibition of SAPK/JNK inhibits STAT1 serine^{727} phosphorylation and IRF-1 activation

To determine if SAPK/JNK is responsible for serine phosphorylation of STAT1 upon IL-27 stimulation JNK inhibitor II, a known inhibitor of this protein, was used. IRF-1 was included to test the importance of SAPK/JNK for IRF-1 expression.

HUVECs were incubated with IL-27 (20ng/mL) and either pre-treated with or without JNK inhibitor II (50µM) for 30 min and STAT1 serine^{727} phosphorylation and IRF-1 expression observed by immunoblotting.

The Western Blot analysis revealed reduced serine^{727} phosphorylation of STAT1 after 30 minutes stimulation with IL-27 in the presence of JNK inhibitor II and this prevailed for the two hours analyzed (Figure 21A, lane 1) revealing that IL-27 regulates serine phosphorylation of STAT1 via activation of SAPK/JNK. In addition it is observed that IRF-1 expression presents a minor decreased (non-significant) when SAPK/JNK is inhibited after one hour of stimulation with IL-27 (Figure 21A, lane 5).

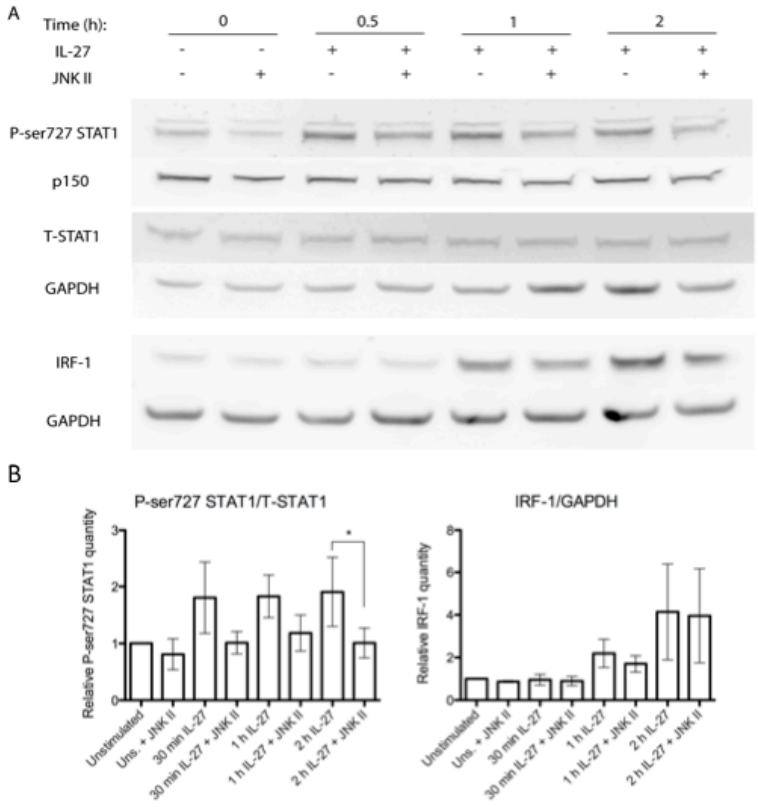

Figure 21: Serine^{727} phosphorylation of STAT1 is reduced by JNK inhibition. HUVEC were pre-treated with JNK inhibitor II (50µM) for 30 min and incubated with IL-27 (20ng/mL). At the indicated time point's cells were lysed by addition of lysis buffer. A: The cellular lysates were used for immunoblotting with antibodies against P-ser727 STAT1, Total STAT1 and Total IRF-1. GAPDH and p150 were used as loading controls. Data are representative of three independent experiments. B: Graphical representation of Western Blot quantification. Mean of three experiments with respective Standard deviation. *: $p < 0,05$ (Bonferroni's post test).

No modification in phosphorylation at serine^{727} of STAT3 upon IL-27 stimulation could be observed (Figure 13), although unstimulated phosphorylation was detectable. To test if SAPK/JNK is involved in the basal level of STAT3 serine phosphorylation we also included an analysis of STAT3 serine^{727} phosphorylation after pre-treatment with JNK inhibitor II.

Once again, the Western Blot analysis showed no alteration in phosphorylation of the serine^{727} residue in STAT3 (Figure 22A and B) after IL-27 stimulation. In addition, no reduction of basal serine phosphorylation was observed after pre-incubation with JNK inhibitor II.

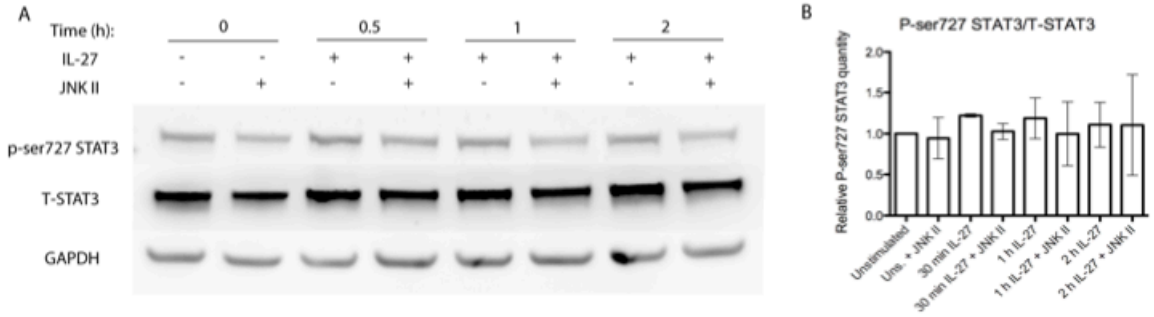

Figure 22: JNK inhibition does not influence basal serine phosphorylation of STAT3. HUVEC were pre-treated with JNK inhibitor II (50µM) for 30 min. Incubation with IL-27 (20ng/mL) for 30 min, 1 h and 2 h. A: Western Blot followed by incubation with antibodies for P-ser727 STAT3 and Total STAT3. GAPDH was used as loading control. Data are representative of three independent experiments. B: Graphical representation of Western Blot quantification. Mean of three experiments with respective Standard deviation. Values do not present statistical significant difference.

GBP2 is activated upon IL-27 stimulation

Very little is known about GBP proteins in endothelial cells. They have been related with inhibition of proliferation and invasion[58]and as tumor supressors[76], but their function is not fully understand. Besides this, we were encouraged to search for a possible role of GBP family in response to IL-27 because these proteins were previously related with STAT1 serine phosphorylated and IRF-1[74,77].

Observations from the laboratory showed GBP2 to be activated after 6 hours with IL-27, and with increased activation from 24 to 48 hours (Appendix 3). Also, knockdown experiments performed with the EA.hy926 cell line, with both siRNA for STAT1 and IFR-1 showed decreased expression of this protein (Appendix 3). These experiments verify GBP2 as a downstream target of STAT1 and IRF-1.

Not much is known about the localization and function of this GBP2, I therefore performed immunofluorescence experiments visualizing GBP2 at 2, 6 and 24 hours after IL-27 stimulation. (Figure 23).

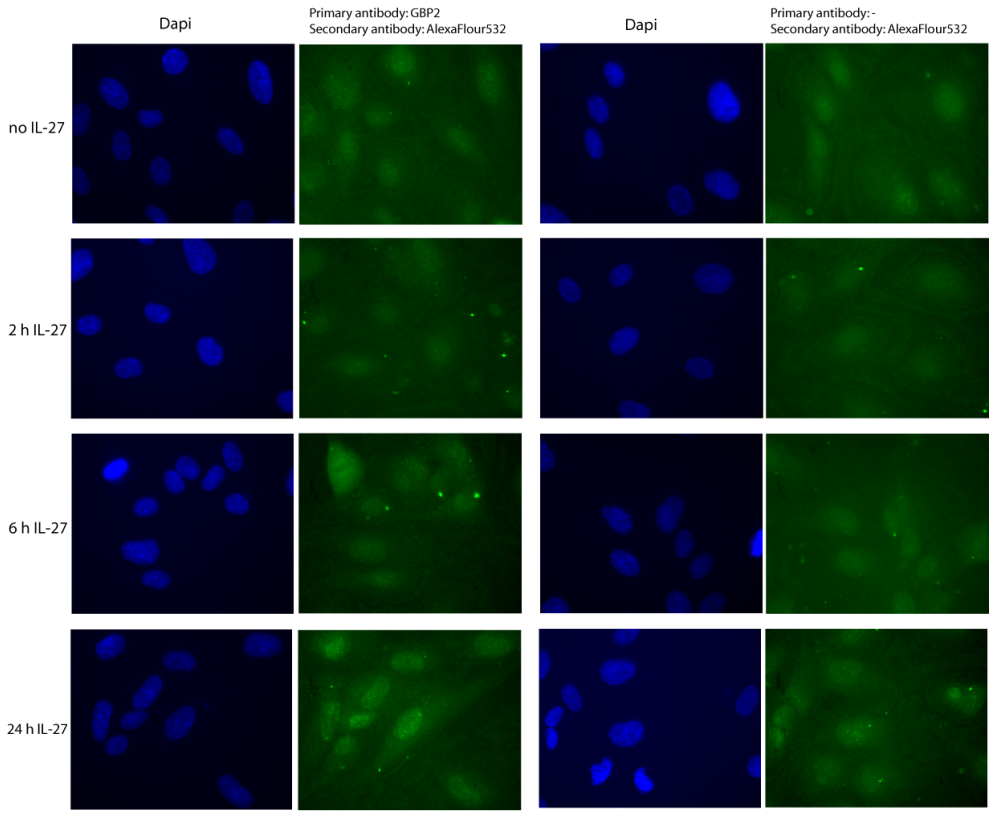

Figure 23: GBP2 is present in the nucleus after 24 hours of stimulation with IL-27. HUVEC incubated for different times with 20ng/mL of IL-27. Incubation with Total GBP2 antibody or PBS alone followed by staining with AlexaFlour532 (green). Nuclei were stained with DAPI (blue).

Unfortunately, it was not possible to obtain a reliable result, since further optimization of antibody concentrations are still needed. Different blocking buffer compositions and different secondary antibodies (AlexaFlour555) have been tested, however, still unsuccessful.

Although the control samples show a high background staining, the results indicate nuclear localization of GBP2 after 24 hours of stimulation with IL-27 (Figure 23).

Sub-project: STAT5 is Tyrosine^{694} phosphorylated after IL-27 stimulation.

STAT5 was recently reported to regulate angiogenesis[54]. It was also shown to be expressed by IL-27 in mice naive CD4^{+} T cells[78].

In order to dissect if STAT5 could play a role in IL-27 signalling in endothelial cells an 8 hours time-course of HUVEC stimulated with IL-27 was performed. Similar to STAT1 tyrosine^{701} phosphorylation (Manuscript under preparation), phosphorylation of STAT5 tyrosine^{694} was observed after 15 minutes of stimulation with IL-27 (Figure 24).

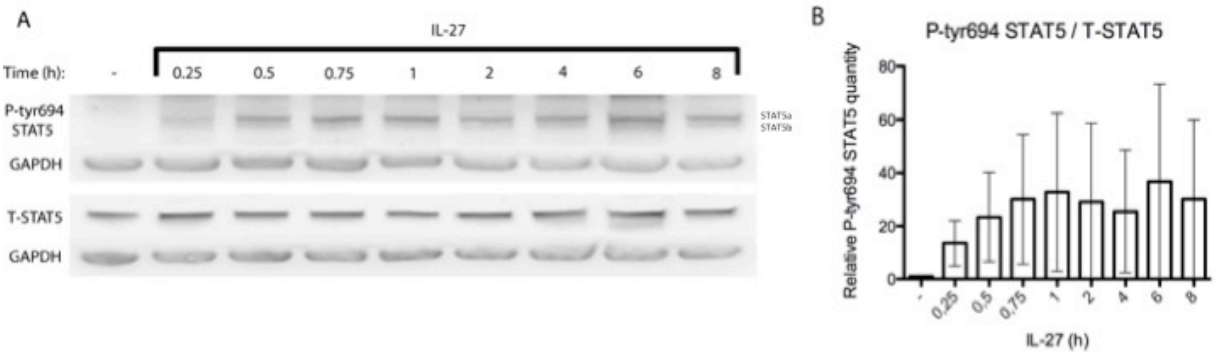

Figure 24: STAT5 tyrosine phosphorylation is induced by IL-27. HUVEC were treated with IL-27 (20ng/mL) and cells were lysed at the time points shown. A: Cellular lysates were used for Immunobloting with antibodies against phosphorylated STAT5 (Tyr694) and Total STAT5. GAPDH was used as loading control. Data are representative of three independent experiments. B: Graphical representation of Western Blot quantification. Mean of three experiments with respective Standard deviation.

Observations from the laboratory about cellular localization of tyrosine^{701} phosphorylated STAT1 showed us that STAT1 is translocated to the nucleus, when phosphorylated at the tyrosine^{701} residue, 15 minutes after stimulation with IL-27 (data not shown). A similar Immunofluorescence experiment, treating cells with antibody against phosphorylated STAT5 in tyrosine^{694}, was performed to observe if nuclear translocation is also underlying potential STAT5-induced transcription.

Phosphorylated STAT5 was already detected in the unstimulated sample. After stimulation with IL-27 a gradual translocation of the phosphorylated protein to the nucleus was observed, being most evident at 2 and 4 hours time-points (Figure 25).

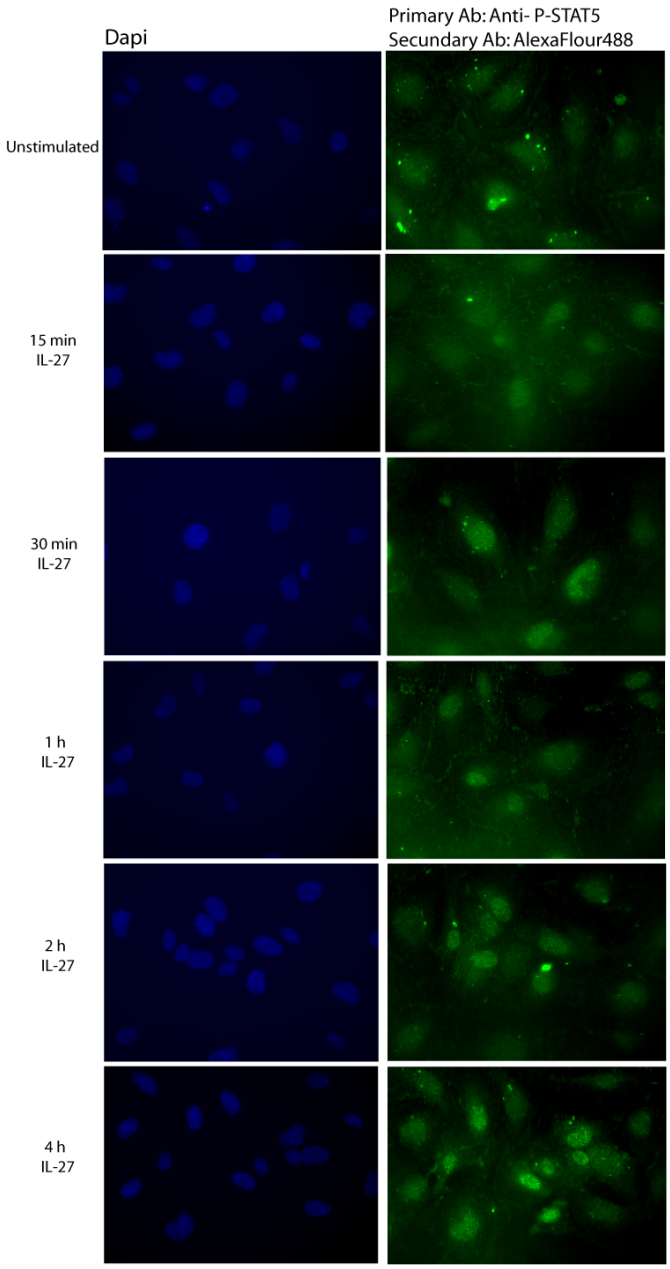

Figure 25: Phosphorylated STAT5 is translocated to the nucleus after IL-27 stimulation. HUVEC were treated with IL-27 (20ng/mL) for the time points shown. After this celles were fixated and incubated with a primary antibody against phosphorylated STAT5 (Tyr694) followed by AlexaFlour488 (green) and DAPI in order to stain the nuclei (blue). Images are representative of two independent experiments.

Angiogenesis Assays

In the second part of my master project I have focused on selection and optimization of different *in vitro* and *in vivo* angiogenesis assays, with the purpose of defining the optimal assay for measuring reliable effects of IL-27 on angiogenesis.

Cell Proliferation Assay

The BrdU assays are often used to determine proliferation rate by measuring BrdU incorporation during S phase. In order to optimized this assay for HUVEC cells I began by testing different cell densities. HUVEC were seeded in the exact cell density required and incubated with BrdU for 6 hours. The absorbance was then read using an ELISA micro-plate reader. It was chosen to use in all next experiments 2000 cells per well, since this is within the linear correlation between absorbance and cell numbers (Figure 26).

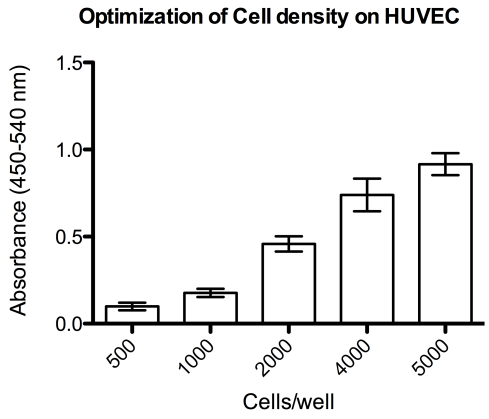

Figure 26: Optimization of HUVEC cell density for BrdU proliferation assay. HUVEC were seeded in complete medium and incubated for 24 hours. BrdU label was added and absorbance measured after 6 hours. N = 2

With the aim of observing a different rate in proliferation of cells treated with IL-27, the next step was to test different concentrations of this cytokine. First, cells were pre-incubated with different concentrations of IL-27 for 24 hours.

Figure 27 indicates that stimulation with 20-100ng/mL IL-27 leads to a small increase in proliferation (although not significant). Since IL-27 has been shown to reduce proliferation of lymphatic endothelial cell, this result was not expected. Instead we had anticipated a decrease in absorbance at least after treatment with 50 and 100ng/mL IL-27. However, paying attention to the initial absorbance values, these are lower compared to the initial experiment (Figure 26) indicating that the experimental conditions were different than the initial experiment (Figure 26).

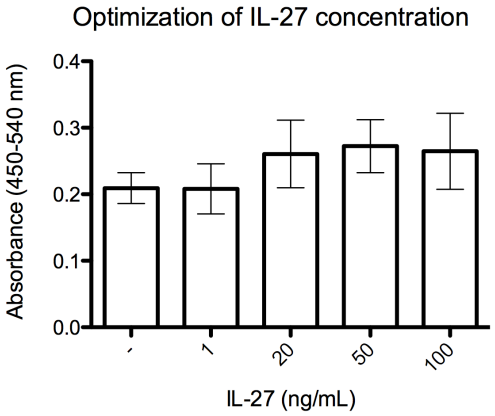

Figure 27: Effect of different IL-27 concentrations on HUVEC proliferation. HUVEC were seeded in complete medium, incubated for 24 hours with IL-27 and absorbance measured after 6 hours of incubation with BrdU label. Number of cells used: 2000 cells/well N = 3

To help us understand the effect of IL-27 on HUVEC proliferation it was decided to reduce the serum level to 2% FBS in the next experiments, thereby reducing the proliferation of non-treated cells. Additionally, FGF, a known stimulator of endothelial cells proliferation, was used as a positive control. In the same way as before, cells were pre-incubated for 24 hours, with either IL-27 or FGF, or a combination of both.

In cells incubated with 50ng/mL FGF an increase in absorbance was observed, compared to control, as expected. However, when cells were incubated with a combination of IL-27 and FGF there was no decrease in absorbance, compared to FGF alone (Figure 28). In addition, compared to the first experiment, all absorbance values were lower. This can be explained by the 2% FBS medium used, since cells do not grow at the same rate when the serum concentration is reduced.

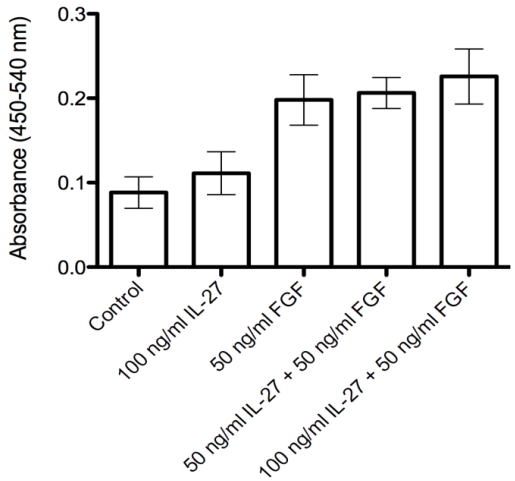

Figure 28: Effect of IL-27 and FGF on HUVEC proliferation. HUVEC were seeded in 2% FBS medium, incubated for 24 hours with IL-27, FGF or a combination of both and 6 hours incubation with BrdU label. Number of cells used: 2000 cells/well N = 2

FGF is a powerful stimulator, and we hypothesized that FGF could mask a possible IL-27 effect, when they were used combined. The third experiment was therefore designed such that cells received IL-27 treatment for 24 hours and after that FGF was added, together with

BrdU for 20 hours. Theoretical in this way, cells could be “programmed” for cell cycle arrest, in response to IL-27.

The results observed show higher values of absorbance; however, comparing with Figure 27 there is no modification in proliferation. The higher absorbance in the control can easily be explained, because cells were incubated for 20 hours with BrdU and not 6 hours as in the previous experiments. In this way more BrdU was incorporated.

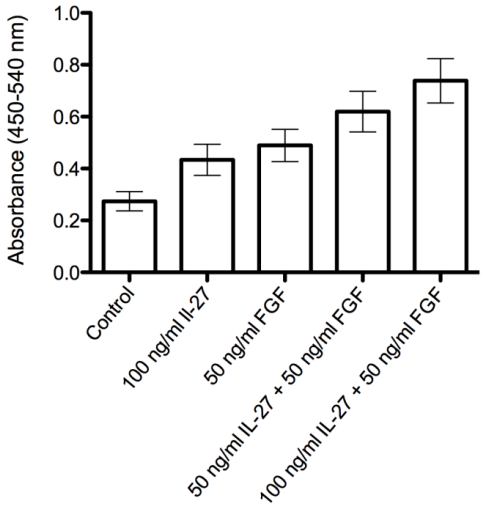

Figure 29: Effect of IL-27 and FGF on HUVEC proliferation. HUVEC were seeded in 2% FBS medium, incubated for 24 hours with IL-27 and for 20 hours with FGF and BrdU label before measuring absorbance. N = 2.

In conclusion, IL-27 does not seem to reduce proliferation of HUVEC cells, but might increase serum and FGF-induced proliferation dependent on the experimental conditions. Further experiments are needed to elucidate the role of IL-27 in proliferation.

Endothelial cells Spheroid-based Angiogenesis Assay

The spheroid assay is a very interesting assay, where we are able to observe cells sprout from an initial spheroid. This method allows us to observe differences in tube formation, according to the stimuli/inhibitor added.

After spheroids assemble, they were incorporated in a collagen matrix and after collagen had polymerized, media with IL-27 at different concentrations were added. With this set up there was no difference in sprouting between the conditions with IL-27 and the control (data not shown).

To carry on the study, we decided to pre-treat cells with IL-27. Basically, while spheroids were assembling, IL-27 was added and spheroids were incubated for about 6 hours. To reveal if pre-treatment was enough to inhibit sprouting, I added medium alone to some wells, and to others medium plus IL-27, at the same concentration as used for pre-treatment.

As can be seen from figure 30 HUVEC formed well assembled and solid spheroids. However, HUVEC spheroids do not seem to sprout. Instead cells migrate individually into the matrix. Furthermore in the centre of the spheroids cells seemed to undergo apoptosis after 24 hours and it was therefore difficult to interpret any result.

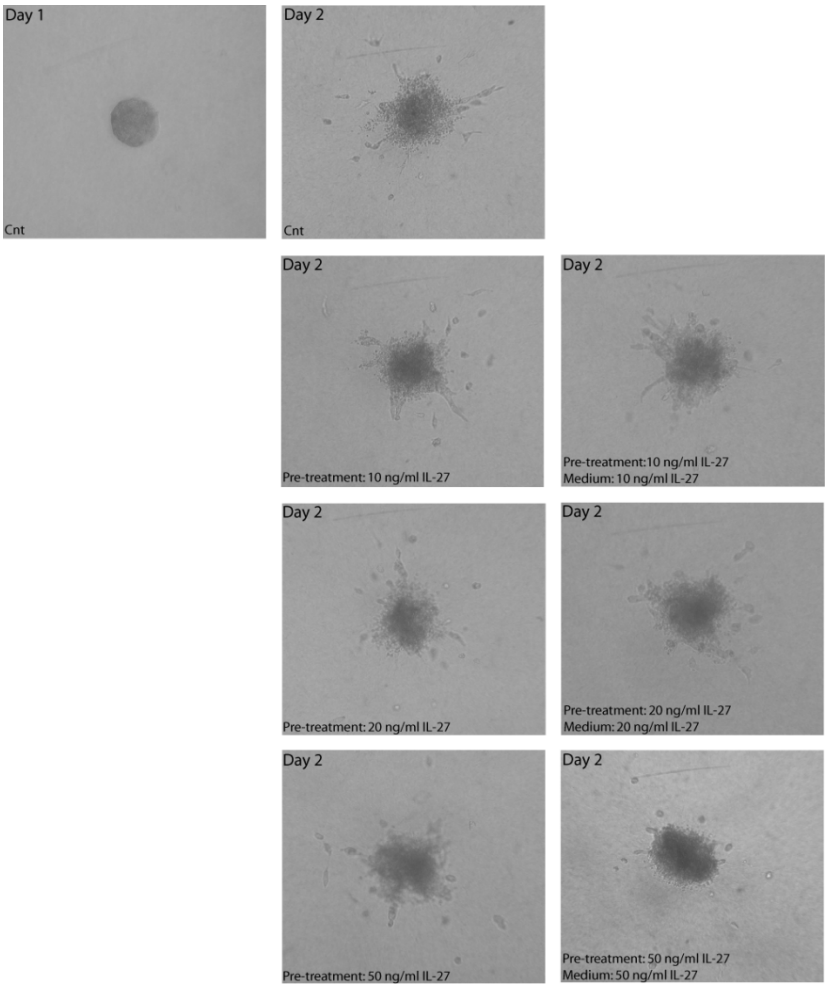

Figure 30: Spheroid Angiogenesis assay using HUVEC cell line. HUVEC spheroids were pre-treated with IL-27 for 6 hours before embedding them in collagen matrix for 24 hours, with or without IL-27 in the medium. Pictures were taken with 10x magnification. N = 2

All in all, HUVEC is a difficult cell line to use with this experimental procedure. It was therefore decided to use the EA.hy926 cell line.

Using the same set up as before, we analyzed spheroids created by EA.hy926 cells. This time it was possible to observe sprouting after 24 hours (Figure 31). Spheroids were also maintaining their structure, although after 48 hours they started disassembling, and the cells in the centre seemed apoptotic (data not shown).

Due to lack of time it was not possible to include all the optimizations this assay still requires.

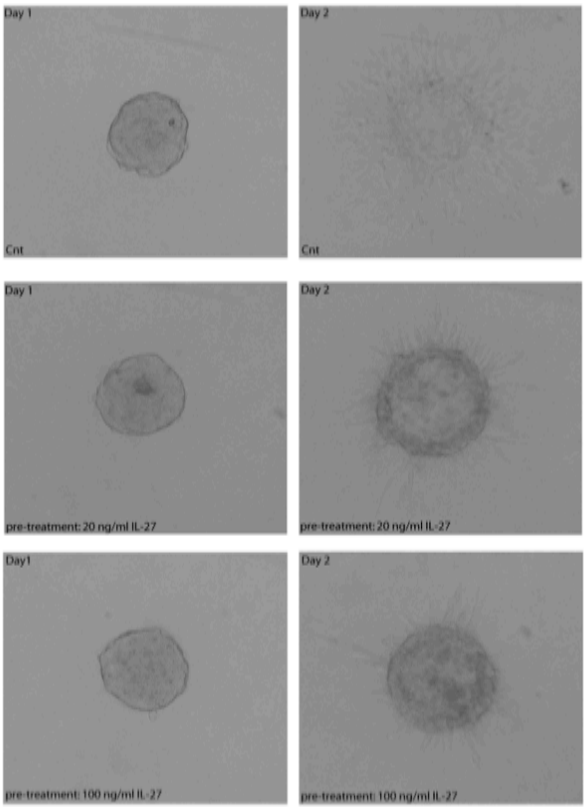

Figure 31: Spheroid Angiogenesis assay using EA.hy926 cell line. EA.hy926 spheroids were pre-treated with IL-27 for 6 hours before they were embedded in collagen matrix for 48 hours, with or without IL-27 in the medium. Pictures were taken after 24 hours with 10x magnification.

Endothelial Tube Formation

Endothelial Tube Formation by use of Matrigel is a model used to study differentiation and modulation of endothelial tube formation in response to angiogenic and/or anti-angiogenic agents.

Similar to the Spheroid-based Angiogenesis Assay, we started by pre-treating cells for 12 hours with IL-27 before they were seeded on the Matrigel. We used different concentrations of IL-27 and in addition FGF as a positive control. Cells were seeded in a 24 well-plate coated with Matrigel in low serum medium, in order to reduce any proliferating stimuli. The experiment was then followed for at least 24 hours.

In the first 2 hours only a few cells had attached to the Matrigel and no tubes had been formed. However, after 6 hours, tube formation had started to occur, but tubes were not complete. It was possible to take quantifiable pictures between 18 and 24 hours.

Figure 32 shows representative pictures of tube formation in different wells stimulated with or without FGF and IL-27. As observed in the figure, it appeared that less tubes had been

formed in both IL-27 treated wells, compared to control. 100ng/mL of IL-27 seemed to be the condition with fewest tubes. However to be certain of these observations is necessary to quantify all the pictures. The FGF treated cells did not seem to form more tubes than the control, but the tubes looked more like a 3D structure, in contrast to the cord-like structures seen in all other condition. The pictures were not quantified because, although attempts were made to take representative pictures of each well, the wells showed a high variation in the number of tubes, depending on the area in the well. In addition, as can be observed in all the pictures lots of cells were present in the medium (dying cells).

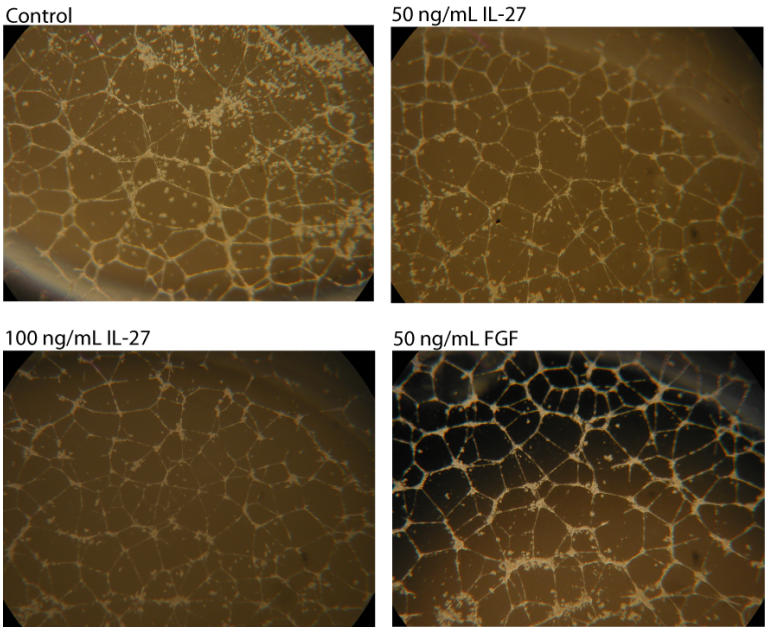

Figure 32: HUVEC used in tube formation assay. Cells were pre-incubated for 12 hours with IL-27 or FGF and seeded on Matrigel at 4x105 cells/mL Pictures taken after 24 hours with 2,5x magnification.

In order to circumvent these problems, we decided to optimize this protocol for a 96 well-plate. By replacing a 24 well-plate with a 96 well-plate, it is possible to take a picture of the entire well, preventing a wrong analysis.

We started by seeding 5 x 10^3 or 1 x 10^4 cell/mL in each well, however we could not observe any tube formation, because there was not sufficient cells. Experiments testing higher cell densities are ongoing.

In vivo Angiogenesis: The mouse Retina Angiogenesis Assay

During my time in the Angiogenesis lab, I had the opportunity to help a colleague (Sebastian Rune Nielsen) with the *in vivo* experiments using the mouse Retina Angiogenesis assay. This assay has provided very interesting results in the angiogenesis field, but it requires some skills, namely knowledge of how to contact and take care of the animals and how to inject and dissect the eye.

The first experiment was an unstimulated time-course, in order to determine exactly when the deep plexus begins to form. It is known from the literature that the deep plexus is formed after the superficial plexus reaches the periphery, after that branches start growing down to other layers[68]. However, the time-course may vary between mouse strains.

Mice were sacrificed starting at postnatal day 6 (P6) until P10 by cervical dislocation. Retinas were dissected and stained for the blood vessels using an antibody against Isolectin.

From figure 33, it can be seen that on post-natal day 6 (P6) the superficial plexus was still under formation, with an angiogenic front in direction towards the periphery of the retina. The deep plexus was nonexistent. At P7 the superficial plexus was completed, however no sign of the deep plexus was observed (the vessels observed in the deep plexus are background from the superficial plexus). Finally, at P8, new vessel formation in the deep plexus was visible and appeared to be completed at P10.

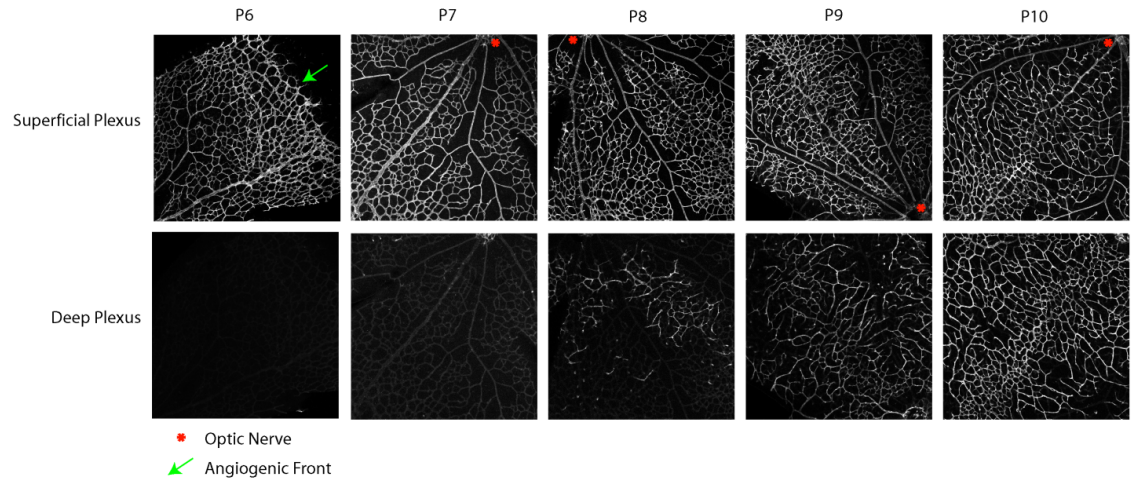

Figure 33: Retinal deep plexus vascularization time-course. Retinas were stained for blood vessels with Isolectin and pictures taken by use of Confocal Microscope.

To determine the effect of IL-27 on vessel formation in the deep plexus the mice should be injected before vascularization is initiated, so we decided to inject the mice at post-natal day 7, and then sacrifice the mice for retina dissection and observation two days after injection, at post-natal day 9.

On postnatal day 7, mice were injected with 1µL rmIL-27 (0.295mg/mL) in the right eye and with 1 µL saline in the left eye for comparison, since there could be variations between different mice. In addition, two mice were left uninjected to reveal if there is any physiological conditions altered due to injection. Mice were then sacrificed by cervical dislocation at P9.

No infection or inflammation was detected after the procedure. Also, there was no difference between saline and uninjected vascularization (data not shown). For all mice a difference in the branch points in the peripheral area could be observed, when comparing IL-27 stimulated vascularization with saline. IL-27 injected retinas had fewer branch points, compared to saline (Figure 34). Consistent with these observations, manual count of branch points from all pictures revealed a significant difference between the two conditions (Figure 33).

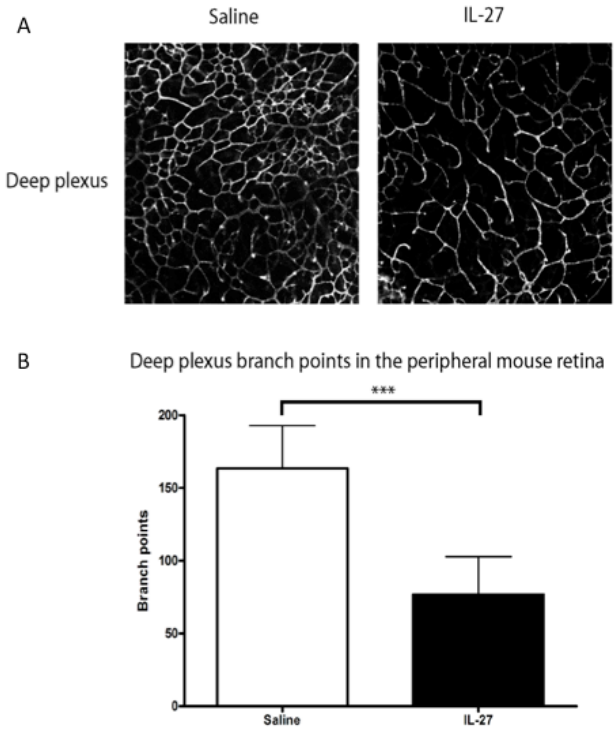

Figure 34: Effect of IL-27 on the peripheral deep plexus vasculature. A: Images are representative of what was observed in mice. Retinas were stained for blood vessels with Isolectin and pictures were taken using a Confocal Microscope. B: Graphical representation of the number of branch points in IL-27 and saline injected eyes. ***: $p < 0,0001$.

Chapter V Discussion

Serine phosphorylation of STAT1 is induced by IL-27

The aim of this first part of the project was to identify the intracellular signalling pathways underlying the physiological effect observed on blood vessels stimulated with IL-27 and focus has been on STAT signalling. It has already been reported in literature that STAT1 and STAT3 mediate opposing effects. STAT1 intracellular signalling mediates an anti-angiogenic effect on HUVECs[45], whereas signalling through STAT3 has a pro-angiogenic effect on human dermal microvasculature endothelial cells[79]. Since, IL-27 presents anti-angiogenic effects on blood vascular and lymphatic endothelial cells[10,18], signalling through STAT1 might be the dominant mediator of IL-27-induced signalling in endothelial cells.

The initial experiments featured in this report show that IL-27 stimulation leads to serine phosphorylation of STAT1 but not STAT3 (Figure 13). Previous results from the laboratory also showed serine[727] phosphorylation of STAT1 in lymphatic endothelial cells (unpublished results), as well as tyrosine phosphorylation of both STAT1 and STAT3 in lymphatic[18] and blood vascular endothelial cells upon IL-27 stimulation (Manuscript under preparation).

IL-27-induced tyrosine phosphorylation has been reported in several cell types[78], and this phosphorylation is essential for the canonical activation of STATs proteins by JAK proteins leading to dimerization, nuclear translocation and consequent transcription of STAT target genes[36]. However, serine phosphorylation is poorly studied. What is the function and which kinase is responsible for the phosphorylation, these questions remain to be answered. Some researchers assert that serine phosphorylation is required to increase transcriptional competence[37,74]. Serine phosphorylation only exists in certain STATs family members, due to a conserved sequence in the C-terminal, known as PMSP motif. In fact, only STAT1α is serine phosphorylated, since STAT1β does not contain this motif[71].

Tyrosine phosphorylation of STAT1 reveals increased phosphorylation of both STAT1α and STAT1β upon IL-27 stimulation, but most pronounced for STAT1α (manuscript under preparation). This suggests that STAT1α is the dominant STAT1 isoform involved in response to IL-27, but additional research is required.

IRF-1 expression is due to IL-27-induced STAT1 Serine727 phosphorylation

Due to lack of knowledge into the mechanism leading to serine phosphorylation and the relevance of this phosphorylation it was decided to address these questions. IRF-1 expression was shown to be dependent on serine^{727} phosphorylation of STAT1 in response to IFNγ in mouse fibroblasts[74,77]. For this reason we decided to test if IRF-1 was a downstream target of STAT1 in IL-27 stimulated endothelial cells. We clearly observed a dramatically increase in IRF-1 expression in endothelial cells after IL-27 stimulation (Figure 14). Yet, to confirm the relation between STAT1 and subsequent IRF-1 expression, a knockdown of STAT1 was performed by Sebastian Rune Nielsen from the laboratory (Figure 15). The results obtained showed an abrupt decrease in IRF-1 expression, in the presence of IL-27, after STAT1 knockdown. These observations clearly show that IRF-1 expression after IL-27 stimulation is dependent on STAT1 activity.

As discussed below, my data point to SAPK/JNK as the kinase responsible for serine phosphorylation of STAT1. A JNK inhibitor was therefore used to determine if serine phosphorylation of STAT1 was necessary for IRF-1 expression to occur. A decrease in IRF-1 protein in JNK inhibitor II treated HUVEC was observed (Figure 21), so the link between STAT1 serine phosphorylation and IRF-1 seems to have been established. However, we should be careful when interpreting these results, as the quantification did not show a significant difference between HUVEC treated with or without the JNK inhibitor. Further experiments will be performed to elucidate this question. In addition, to complement these results we could perform an mRNA level analysis of IRF-1 after cells being treated with or without the JNK inhibitor and stimulated with IL-27.

IRF-1 is localized in the nucleus after IL-27 stimulation

STAT1 is known to translocate to the nucleus upon tyrosine phosphorylation[33,35,36]. In IL-27 context, our laboratory has shown STAT1 nuclear translocation in HUVECs when STAT1 was phosphorylated at both tyrosine^{701} and serine^{727} (data not shown). Besides, it is known that IRF-1 is constitutively in the nucleus[57]. Our data also revealed that IRF-1 is localized in the nucleus upon IL-27 stimulation. We observed, even in the unstimulated sample, the presence of IRF-1 in the nucleus, however it was evident that IRF-1 expression was increased after 1 hour with IL-27 (Figure 16), matching the results observed for the protein expression (Figure 14).

In conclusion, we are confident that IRF-1 is a downstream target of STAT1 in IL-27 stimulated endothelial cells, and that IRF-1 is translocated to the nucleus after translation and remains there to exert its function.

P38 does not phosphorylate STAT1 at Serine residue after IL-27 stimulation

In order to get a mechanistic insight into how STAT1 is serine phosphorylated we looked for the responsible kinase. Several MAPKs have been reported to phosphorylate STAT1[41,44] and the PMSP motif present in STATs is similar to the MAPK recognition consensus sites[71].

One such kinase is p38[37,77], although it is possible that this relation is only observed for specific types of stimuli. In the case of UV irradiation there is a clear relation between p38 and STAT1[77]. The physiological effect of p38 is balanced due to activation of different p38 isoforms, depending on the pro- or anti-apoptotic signal. For instance, TGF-β1, a multifunctional growth factor, which induces vessel formation but inhibits endothelial cell proliferation and migration, was shown to induce p38α leading to apoptosis. In contrast, VEGF, which stimulates endothelial cell proliferation and survival, activates p38β, which is anti-apoptotic[80]. This reinforces the selective activation of each p38 isoform, depending on the cytokine or growth factor involved. Because of this we choose to test potential IL-27 induced expression of all p38 isoforms.

P38α is pro-apoptotic, so we expected that this isoform would respond to IL-27 stimulation. We can in fact observe a tendency of higher expression of p38α after IL-27 stimulation (Figure 17). However, immunoblotting had variations in GAPDH protein expression and the protein expression left inconclusive results.

We decided to proceed with p38 analysis through mRNA level of expression. This is a very reliable method, when all optimizations are performed accurately. Is also necessary to understand what kind of errors might occur when Real-Time PCR is performed and always provide the necessary controls for the experiment. We started by selecting which was the best p38α primer pair, from the four pair existing. Based on the experimental knowledge from the laboratory, I performed all the steps for optimization of the method using the Reverse Transcription (RT) kit from Qiagen (Omniscript® RT kit). However, we came across with poor efficiency values for the standard curves (data not shown). It came to our

knowledge that it was possible that the reverse transcriptase was not inactivated in the first step of the Real-Time PCR, which led to overestimation of amplification efficiency[72]. It was therefore decided to use a new RT kit (Phusion RT-PCR kit, from Finnzymes, which already includes an RT inactivation step (Methods). With this new set up acceptable efficiency values for each standard curve (p38α and GAPDH primers) were obtained.

The analysis of mRNA level still showed no p38α response after IL-27 stimulation. In conclusion, although this MAPK is activated by inflammatory cytokines[28] and has been shown to act in endothelial cells, it does not appear to be activated in HUVEC, upon IL-27 stimulation (Figure 18). It is possible that further research would reveal that other p38 isoforms are involved in IL-27 signalling, since previous data obtained by our group using antibodies targeting phosphorylation of all p38 isoforms showed increased phosphorylation when HUVEC where stimulated with IL-27 (data not shown).

SAPK/JNK induces STAT1 Serine^{727} phosphorylation

P38 is not the only stress activated MAPK. SAPK/JNK was the first stress-activated MAPK discovered, and it is already recognized as the link between UV irradiation or inflammatory signaling, like TNF-α and LPS and STAT3 serine^{727} phosphorylation[37]. Recently, it was also shown that SAPK/JNK regulates HUVEC angiogenesis, namely tube formation and cell proliferation, in response to epidermal growth factor (EGF)[22].

I further investigated the possible role of SAPK/JNK in IL-27 signalling by examining the SAPK/JNK protein phosphorylation pattern. A different pattern in phosphorylation of each SAPK/JNK isoform was observed when looking at the western blot, although quantification of the data showed no significant rise (Figure 19). Quantification was done by normalization of the phosphorylated SAPK/JNK protein against p150. It could be interesting to analyze the expression level of the SAPK/JNK proteins since changes in the protein levels with time could mask changes in phosphorylation.

Consistent with the SAPK/JNK being responsible for serine phosphorylation of STAT1 pre-incubation with JNK inhibitor II of IL-27 stimulated HUVEC led to reduced serine phosphorylation of STAT1 (Figure 21).

It is possible that the response to IL-27 of each isoform is different, and maybe only one of them is required for STAT1 activation. The involvement of JNK1 (p46 isoform) in Age-

related Macular Degeneration (AMD) has been shown in a recent study. This disease causes blindness in developed countries and is characterized by growth of blood vessels from the choroid toward the retina called choroidal neovascularization (CNV). When JNK1 was inhibit there was a reduction in CNV, with decreased apoptosis and increased VEGF expression[30]. The SAPK/JNK data indicate that the p46 isoform was more prone to phosphorylation than p54 isoform (Figure 19) and that there is no redundancy between the isoforms.

Theoretically, since the phosphorylation of serine^{727} of STAT1 is observed after 15 minutes with IL-27, we could assume that JNK1 (p46 isoform) is the responsible kinase since it is phosphorylated at the same time point (15 minutes, Figure 19). In order to test this, siRNA targeting either isoform could be a relevant tool.

Until now, there is no information about SAPK/JNK localization after phosphorylation, which was the reason for us to perform immunofluorescence experiments. Several optimization steps were required, with different blocking buffers and different secondary antibodies, as the control sample (with no primary antibody) presented high background (data not shown). Surprisingly, phosphorylated SAPK/JNK appeared as dots, which might indicate this protein is present in vesicles. However, it is not possible to identify an accurate organelle, since the dots are present all over the cell (Figure 20). In addition, no difference in fluorescence intensity was observed throughout the time points examined, but it is of note that 24 hours of IL-27 stimulation led to an intense nuclear localization (Figure 20, last row). In conclusion, further investigation is needed to elucidate the localization of phosphorylated SAPK/JNK and to determine whether this kinase is present in vesicles or the “dots” simply represent an artefact.

It is possibly that we do not detect an alteration in the phosphorylation pattern in SAPK/JNK because the antibody used targets the two isoforms, and for that the rise and decrease in the phosphorylation of each isoform could be outbalanced. However, this observation reinforces the idea that only one isoform could be responsible for STAT1 serine^{727} phosphorylation. It would be interesting, to target each isoform autonomously, and if possible to address for the localization of each independently. Another way of verifying this hypothesis would be to immunoprecipitate STAT1 phosphorylated at serine^{727} and then to do immunobloting for each JNK isoform.

Also, it would be interesting to further investigate what is the function of phosphorylated SAPK/JNK in the nucleus after a 24 hours stimulus with IL-27, since so far, we

do not know what the function of SAPK/JNK in the nucleus could be at this time point. It is known that JNK translocate to the nucleus due to other stimuli, for instance, JNK was found to translocate from the cytoplasm to the nucleus after IL-1 stimulation[81] in fibroblast-like synoviocytes.

STAT3 showed no response to SAPK/JNK inhibition or to IL-27 stimulation, so although serine phosphorylation of this protein has been linked to SAPK/JNK[42,43], it seems that STAT3 serine phosphorylation is induced by IL-27-regulated SAPK/JNK activity.

GBP2 expression is linked to STAT1 and IRF-1 activity after IL-27 stimulation

In the literature we find several links between STAT1 serine phosphorylation and IRF-1 expression. In response to IFNγ, a cooperative action of STAT1 serine[727] and IRF-1 regulates the GBP2 promoter in Bone marrow-derived macrophages[74]. A decrease in GBP1 gene expression when serine[727] of STAT1 was mutated in mouse fibroblasts has also been reported[77]. Both references associate the GBP family to STAT1 phosphorylated at serine727 and IRF-1 expression, which motivated us to search for a possible role of this GBP protein family in response to IL-27.

Experiments performed by Sebastian Rune Nielsen from the laboratory showed GBP1 and GBP2 activation after 6 hours and increasing with time in the presence of IL-27, but most evident for GBP2 (Appendix 3). To validate the connection between STAT1/IRF-1 and GBP1 and GBP2 a knockdown experiment was performed using siRNA specific for STAT1 and IFR-1. These experiments showed a decrease in the expression of both GBP1 and GBP2, once again, most evident for GBP2 (Appendix 3). This assured us about the activation of GBPs in response to IL-27 and clearly revealed the importance of STAT1 and IRF-1 in GBP expression.

To understand the function of GBP2 (since this was the protein that showed higher expression) we started by examine its cellular localization. After 24 hours stimulation with IL-27, GBP2 was primarily localized in the nucleus(Figure 23); however, these experiments require further optimization, due to high background in control samples.

Very few studies describe the function of GBPs in endothelial cells. However, there are several indications from previous studies that GBP1 exert antiangiogenic function in endothelial cells through inhibition of MMP-1, leading to inhibition of cell proliferation and invasion[58,61–63]. GBP2, in turn is known to inhibit TNF-α-induced expression of MMP-9, in NIH

3T3 fibroblasts[82]. Our ongoing studies will reveal whether IL-27 regulates angiogenesis via GBP-mediated downregulation or metalloproteinases.

IL-27 induces STAT5 Tyrosine^{694} phosphorylation

We decided to determine if IL-27 regulates phosphorylation of STAT5 because IL-27 has been shown to regulate STAT5 in in mice naive $CD4^+$ T cells[78].

It was rather interesting to observe that STAT5 showed a phosphorylation and localization pattern similar to STAT1 (Figures 24 and 25). It was also interesting to observe that there is a higher rate of tyrosine^{694} phosphorylation in STAT5a, which indicates that only this protein member is linked to angiogenesis.

It is known that STAT5 can regulate cell cycle progression[51] and when stimulated by FGF2 and FGF8b induce migration of mouse brain endothelial cells[53.] It is therefore possible that when endothelial cells are stimulated with IL-27, phosphorylation of STAT5 would lead to enhanced cell migration. To be certain of this statement we could use Wound-healing assay in combination with STAT5 knockdown or inhibition.

With these preliminary results, it is imperative to further investigate the function and regulation of STAT5 tyrosine^{694} phosphorylation in angiogenesis.

Angiogenesis Assays

Angiogenic assays offer indispensable support to investigate how physiological and pathological angiogenesis occurs. Moreover, they provide useful information about the effect of pro- and anti-angiogenic factors. But until now no assay alone can answer questions from molecular patterns to morphological. In order to obtain the maximum benefit from angiogenic assays it is therefore required to perform multiple different tests. I have tested and optimized several *in vitro* assays in parallel, with the intent that these assays could help us understand how IL-27 affects angiogenesis in future studies. These experiments are ongoing, but I will try to discuss the benefits of each assay.

Proliferation assay based on BrdU method

Due to a previous paper from the laboratory, showing IL-27 mediated reduction of lymphatic endothelial cells proliferation, we expected IL-27 to also inhibit HUVEC proliferation. However, no inhibitory effect on proliferation by IL-27 could be detected by use of the BrdU method (Figures 28 and 29). This is a very sensitive method but there were high disparities between wells with the same conditions, which could be affecting the interpretation.

The high disparities can be explained by several factors. First thing that requires attention is that an increase in DNA labelling can also be due to DNA repair. In contrast, decrease in labelling might be due to a cytotoxic effect[64]. Also, the use of different HUVEC passages in the various experiments could have influenced the output of the experiments. HUVEC is a primary line, which suffers modifications in function rapidly, and eventually becomes senescent. Another limiting factor is the cell confluency. Although we always seeded the same cell number, we could not be certain that all replicates would behave the same way, which introduce a higher degree of variance in the results of each experiment.

When performing a revision of the literature several proliferation assays have been reported[64,65], some rely on cell count and in others it is even possible to identify cell death. To obtain the most accurate result more than one proliferation assay could be combined. Alternatively, or in combination with the BrdU Proliferation assay, we can do a cell cycle analysis using flow cytometry. In fact, collaborators from the laboratory are already performing this. By analysis of the DNA content of cells, it is possible to measure the percentage of cells in each cell cycle phase.

Although all the statements presented before can explain the inconsistent results observed with the different set ups done for the proliferation assay, we should note that cells in culture do not behave as cells *in vivo*. Endothelial cell cultures already are in a proliferating state in contrast to quiescent endothelial cells in an established *in vivo* vasculature[65]. In addition, it is possible that we do not see an effect simply because IL-27 does not exert an effect on proliferation.

Endothelial cells Spheroid-based Angiogenesis Assay

We performed the Endothelial cells Spheroid-based Angiogenesis Assay in order to determine a possible effect of IL-27 on sprouting, that is whether this cytokine would affect migration, invasion and tube formation, important processes during angiogenesis. However,

this method requires further optimization before we can make any conclusions about L-27 regulated sprouting.

It is necessary to optimize the method; however, our preliminary results as well as evidences from the literature show that this assay is better to use in combination with pro-angiogenic factors than anti-angiogenic factors. Korff and Augustin showed in 1999 that HUVEC presented a low baseline angiogenic activity, requiring stimulation with exogenous cytokines and thus, appeared to be more suitable for analysis of pro-angiogenic substances. On the other hand, Bovine Aortic Endothelial cells (BAEC) were capable of proliferating without exogenous cytokines and in low serum, making them suitable for inhibitory studies[66].

My results showed that HUVEC is not a suitable cell line for this assay because the HUVEC spheroids did not form sprouts (Figure 30). Also, this endothelial cell line does not seem to be able to survive for more than a few hours in the collagen matrix, which makes it impossible to obtain a quantifiable and reliable result. Perhaps, if we try to add a growth factor, for instance FGF, we will observe a completely different pattern.

Nevertheless, our aim was to understand the effect of IL-27 and we therefore switched to another cell line. We need to be careful when choosing this cell line for the studies, since a non-human cell line or even a human endothelial cell line of different origin can respond differently to distinct stimuli. Because of this we choose to continue with the EA.hy926 cell line, which is comparable to HUVEC. Also more resistant to extreme conditions, so we predicted it could survive for a longer time period in the collagen matrix. These experiments are ongoing, yet it is already possible to say that the EA.hy926 cell line after 24 hours presented quantifiable sprouts (Figure 31).

Endothelial tube formation assay

The Endothelial Tube Formation was one of the first assays developed to study angiogenesis, and for that many research groups use it to study the effect of different pro- and anti-angiogenic factors. Yet, an attentive preparation and careful quantification of the results is needed.

Data indicate there is a reduction of the tube formation when cells were treated with IL-27 (Figure 32). The experiments performed did not allow for quantification, simply because of the less than optimal quality. In addition, the control presented a high amount of dead cells. Since FGF is a pro-angiogenic factor, we expected to observe an increase in tube formation.

However, the number of tubes appeared to be similar to the control, but morphologically, FGF-treated HUVEC appeared to form more solid and robust tubes (Figure 32).

Yet, because the experiment indicates changes in the cell response due to IL-27 stimulation, we will further improve this method for future experiments.

By improving the cell density, possibly we can optimize the cell growth conditions. Also, using a 96-well plate to perform the assay will allow us to take pictures of the entire well. By this, the quantification will be as exact as possible.

Future work will also include new conditions, where we will test the medium used for pre-treatment of cells seeded on the Matrigel. We believe that during pre-incubation several anti-angiogenic factors are released from the HUVEC and that these can also influence in the response. We would like to test this effect on the tube formation and if this assumption reveals accurate we will look in detail which are the anti-angiogenic factors released.

Besides the plans for improving the assay and the experimental set up, we need to keep in mind several aspects already observed by other colleagues. One important step is to be certain of the Matrigel protein concentration. Variations in this will affect the sensitivity of the cells and it will modify their response. A precise protein concentration of 10mg/mL is ideal to perform the assay[67]. Also, this assay does not mimic the real vessel structure, usually the cells organize as a cord like-structure lacking the lumen[64]. Furthermore, there is some debate about the fidelity of the assay, because non-endothelial cells like fibroblasts have been shown to be capable of creating tubes in the Matrigel[65]. In conclusion, this assay should be used in combination with other angiogenesis assays as discussed previously.

Mouse Retina Angiogenesis assay

We started optimizing the mouse Retina Angiogenesis Assay in order to understand angiogenesis *in vivo*. By *in vivo* experiments we will get a better insight into what is the actual effect of IL-27.

In all IL-27 injected mice in each trial performed there was a reduction in branch points of the deep plexus comparing to control (Figure 34). From this we can conclude that IL-27 reduced or delayed vasculature development of retinal deep plexus.

As in all *in vivo* assays, there are some variables we need to pay attention to, namely the differences in development that each animal may present. There might be some mice which present defective development, either due to a physiological problem or maybe due to

lack of aliment, since the first two weeks the pups are kept with the mother and are still nursed.

The mouse Retina Angiogenesis Assay seems to be a promising method to study angiogenesis *in vivo*. After full optimization, it will be possible to carry on the study staining the retina for proteins like phosphorylated STAT1 or IRF-1. This might lead us to identify protein patterns between the tip cells and stalker cells. Also, we can in the future determine the effect of STAT1 or IRF-1 knockdown on angiogenesis *in vivo*. Angiogenesis assays are useful for screening of pro- and anti-angiogenic agents, taking them to clinical trials for the treatment of many angiogenesis related diseases, like diabetes, macular degeneration and cancer[64]. But angiogenesis assays are also useful tools to investigate signalling pathways and thereby identify potential therapeutic targets. However, we need to take in account all the limiting steps of each assay, and avoiding over interpretations.

To screen potential targets, *in vitro* assays are very helpful, however it is required to adjust the culture conditions so they mimic the *in vivo* situation. In the Endothelial Tube Formation assay, if endothelial cells are co-cultured with mural cells there will be a closer proximity to *in vivo* models. Mural cells are recruited after endothelial cells have emerged to form tubules, to maintain vessel quiescence and stability[64]. An essential step of angiogenesis study is in fact interaction between mural and endothelial cells.

Regardless of the quantity of data that an *in vitro* assay generates, *in vivo* assays are an absolute requisite. *In vivo* assays are still difficult to perform and tend to require surgical skills[65]. A single *in vivo* model is not sufficient to fully explore angiogenesis as there are variations between species, localization of organs or the specific microenvironment[64]. To complement the experiments already performed we could use a tumor model. Implantation of tumor cells is one of the easiest methodologies to investigate angiogenesis during tumor growth[64].

In conclusion, a successful signalling angiogenesis study comprises several *in vitro* assays, designed in a way to investigate different steps of the angiogenesis process, followed by more than one *in vivo* assay.

Chapter VI General Conclusions and Future Perspectives

This study provided evidence that IL-27 induces phosphorylation of the stress activated MAPK SAPK/JNK, which in turn induces STAT1 serine^{727} phosphorylation. This serine phosphorylation of STAT1 is necessary for expression of IRF-1. In addition, the data reveal that STAT1 is responsible for expression of the anti-angiogenic GTPases GBP1 and 2. The *in vitro* experiments still need optimization before the effect of IL-27 on angiogenic processes *in vitro* can be determined. However, the *in vivo* experiments clearly show the pronounced effect of IL-27 on angiogenesis.

There are still many questions to address. We can start by asking which are the MAPKK and MAPKKK responsible for SAPK/JNK activation. It is also important to understand how STAT1 regulates expression of IRF-1 and GBP1/2. Is STAT1 translocated to the nucleus as homodimers or heterodimers? Are there any cofactors involved in transcription initiation? And what is the function of GBPs in IL-27 regulated angiogenesis.

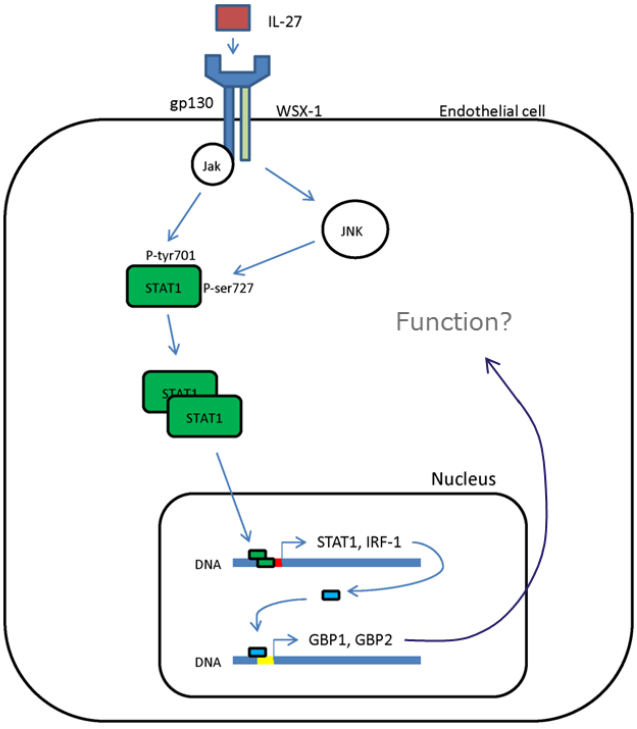

Figure 35: Scheme of proposed IL-27 intracellular signalling in endothelial cells.

In summary:

- Upon IL-27 stimulation of HUVEC, STAT1 is phosphorylated at Serine^{727} by SAPK/JNK, and this leads to activation of IRF-1 expression, which in turn activates GBP2 gene transcription.
- The Endothelial cell tube formation assay indicates a reduction in tube formation when HUVEC are stimulated with IL-27, for both concentrations tested (50ng/mL and 100ng/mL).
- Retinal deep plexus vascularization in mice is reduced by IL-27.
- STAT5a is phosphorylated at Tyrosine^{694} after IL-27 stimulation in HUVEC.

Future experiments:

- Investigate IL-27-induced formation of STAT1 homo- and heterodimers.
- Further investigate the effect of IL-27 and STAT1 on cell cycle progression, using Flow Cytometry.
- Use the Mouse Retina Assay to understand STAT1 and IRF-1 function in *in vivo* angiogenesis, through tissue staining and protein knockdown.
- Try to understand GBP2 function in HUVEC, and its relation to Angiogenesis.
- Continue investigation of STAT5 in relation to angiogenesis in endohelial cells.
- Optimize both the 3D-Spheroid based Angiogenesis Assay and Endothelial cell tube formation assay, in order to determine the importance of STAT1/5, IRF-1 and GBP1/2 in IL-27-regulated angiogenesis.

Chapter VII References

1. Ichihara, E., Kiura, K. & Tanimoto, M. Targeting angiogenesis in cancer therapy. *Acta medica Okayama* **65,** 353–62 (2011).

2. Shojaei, F. Anti-angiogenesis therapy in cancer: current challenges and future perspectives. *Cancer letters* **320,** 130–7 (2012).

3. Greenberg, D. a & Jin, K. From angiogenesis to neuropathology. *Nature* **438,** 954–9 (2005).

4. Carmeliet, P. Angiogenesis in life, disease and medicine. *Nature* **438,** 932–6 (2005).

5. Hanahan, D. & Weinberg, R. A. Hallmarks of cancer: the next generation. *Cell* **144,** 646–674 (2011).

6. Bergers, G. & Benjamin, L. E. Tumorigenesis and the angiogenic switch. *Nature reviews. Cancer* **3,** 401–10 (2003).

7. Pietras, K. & Ostman, A. Hallmarks of cancer: interactions with the tumor stroma. *Experimental cell research* **316,** 1324–31 (2010).

8. Ferrara, N. & Kerbel, R. S. Angiogenesis as a therapeutic target. *Nature* **438,** 967–74 (2005).

9. Wojno, E. D. T. & Hunter, C. a. New directions in the basic and translational biology of interleukin-27. *Trends in immunology* **33,** 91–7 (2012).

10. Shimizu, M. *et al.* Antiangiogenic and antitumor activities of IL-27. *Journal of immunology (Baltimore, Md. : 1950)* **176,** 7317–24 (2006).

11. Pflanz, S. *et al.* IL-27, a heterodimeric cytokine composed of EBI3 and p28 protein, induces proliferation of naive CD4(+) T cells. *Immunity* **16,** 779–90 (2002).

12. Pflanz, S. *et al.* WSX-1 and glycoprotein 130 constitute a signal-transducing receptor for IL-27. *Journal of immunology (Baltimore, Md. : 1950)* **172,** 2225–31 (2004).

13. Takeda, A. *et al.* Cutting edge: role of IL-27/WSX-1 signaling for induction of T-bet through activation of STAT1 during initial Th1 commitment. *Journal of immunology (Baltimore, Md. : 1950)* **170,** 4886–90 (2003).

14. Hibbert, L., Pflanz, S., De Waal Malefyt, R. & Kastelein, R. A. IL-27 and IFN-alpha signal via Stat1 and Stat3 and induce T-Bet and IL-12Rbeta2 in naive T cells. *Journal of interferon cytokine research the official journal of the International Society for Interferon and Cytokine Research* **23,** 513–522 (2003).

15. Kamiya, S. *et al.* An indispensable role for STAT1 in IL-27-induced T-bet expression but not proliferation of naive CD4+ T cells. *Journal of immunology (Baltimore, Md. : 1950)* **173,** 3871–7 (2004).

16. Batten, M. *et al.* Interleukin 27 limits autoimmune encephalomyelitis by suppressing the development of interleukin 17-producing T cells. *Nature immunology* **7,** 929–36 (2006).

17. Hasegawa, E. *et al.* IL-27 inhibits pathophysiological intraocular neovascularization due to laser burn. *Journal of leukocyte biology* **91,** 267–73 (2012).

18. Nielsen, S. R. *et al.* IL-27 inhibits lymphatic endothelial cell proliferation by STAT1-regulated gene expression. *Microcirculation (New York, N.Y. : 1994)* (2013). doi:10.1111/micc.12055

19. Cao, Y., Doodes, P. D., Glant, T. T. & Finnegan, A. IL-27 Induces a Th1 Immune Response and Susceptibility to Experimental Arthritis. *The Journal of Immunology* **180,** 922–930 (2008).

20. Cocco, C. *et al.* Interleukin-27 acts as multifunctional antitumor agent in multiple myeloma. *Clinical cancer research : an official journal of the American Association for Cancer Research* **16,** 4188–97 (2010).

21. Kyriakis, J. M. & Avruch, J. Mammalian mitogen-activated protein kinase signal transduction pathways activated by stress and inflammation. *Physiological reviews* **81,** 807–69 (2001).

22. Shen, K., Sheng, Y., Ji, L. & Wang, Z. Involvement of c-Jun N-terminal kinase and extracellular signal-regulated kinase 1/2 in EGF-induced angiogenesis. *Cell biology international* **34,** 1213–8 (2010).

23. Matsumoto, T., Turesson, I., Book, M., Gerwins, P. & Claesson-Welsh, L. p38 MAP kinase negatively regulates endothelial cell survival, proliferation, and differentiation in FGF-2-stimulated angiogenesis. *The Journal of cell biology* **156,** 149–60 (2002).

24. Jazirehi, A. R., Wenn, P. B. & Damavand, M. Therapeutic implications of targeting the PI3Kinase/AKT/mTOR signaling module in melanoma therapy. *American journal of cancer research* **2,** 178–91 (2012).

25. Cuenda, A. & Rousseau, S. p38 MAP-kinases pathway regulation, function and role in human diseases. *Biochimica et biophysica acta* **1773,** 1358–75 (2007).

26. Cuadrado, A. & Nebreda, A. R. Mechanisms and functions of p38 MAPK signalling. *The Biochemical journal* **429,** 403–17 (2010).

27. Ono, K. & Han, J. The p38 signal transduction pathway: activation and function. *Cellular signalling* **12,** 1–13 (2000).

28. Enslen, H., Brancho, D. M. & Davis, R. J. Molecular determinants that mediate selective activation of p38 MAP kinase isoforms. *The EMBO journal* **19,** 1301–11 (2000).

29. Wagner, E. F. & Nebreda, A. R. Signal integration by JNK and p38 MAPK pathways in cancer development. *Nature reviews. Cancer* **9,** 537–49 (2009).

30. Du, H. *et al.* JNK inhibition reduces apoptosis and neovascularization in a murine model of age-related macular degeneration. *Proceedings of the National Academy of Sciences of the United States of America* **110,** 2377–82 (2013).

31. Johnson, G. L. & Lapadat, R. Mitogen-activated protein kinase pathways mediated by ERK, JNK, and p38 protein kinases. *Science (New York, N.Y.)* **298,** 1911–2 (2002).

32. Roskoski, R. ERK1/2 MAP kinases: structure, function, and regulation. *Pharmacological research : the official journal of the Italian Pharmacological Society* **66,** 105–43 (2012).

33. Reich, N. C. & Liu, L. Tracking STAT nuclear traffic. *Nature reviews. Immunology* **6,** 602–12 (2006).

34. Calò, V. *et al.* STAT proteins: from normal control of cellular events to tumorigenesis. *Journal of cellular physiology* **197,** 157–68 (2003).

35. Haura, E. B., Turkson, J. & Jove, R. Mechanisms of disease: Insights into the emerging role of signal transducers and activators of transcription in cancer. *Nature clinical practice. Oncology* **2,** 315–24 (2005).

36. Levy, D. E. & Darnell, J. E. Stats: transcriptional control and biological impact. *Nature reviews. Molecular cell biology* **3,** 651–62 (2002).

37. Decker, T. & Kovarik, P. Serine phosphorylation of STATs. *Oncogene* **19,** 2628–37 (2000).

38. Chung, J., Uchida, E., Grammer, T. C. & Blenis, J. STAT3 serine phosphorylation by ERK-dependent and -independent pathways negatively modulates its tyrosine phosphorylation. *Molecular and cellular biology* **17,** 6508–16 (1997).

39. Su, L., Rickert, R. C. & David, M. Rapid STAT Phosphorylation via the B Cell Receptor: MODULATORY ROLE OF CD19. *J Biol Chem* **274,** 31770–31774 (1999).

40. Yamashita, H. Differential Control of the Phosphorylation State of Proline-juxtaposed Serine Residues Ser725 of Stat5a and Ser730 of Stat5b in Prolactin-sensitive Cells. *Journal of Biological Chemistry* **273,** 30218–30224 (1998).

41. David, M. *et al.* Requirement for MAP kinase (ERK2) activity in interferon alpha- and interferon beta-stimulated gene expression through STAT proteins. *Science* **269,** 1721–1723 (1995).

42. Lim, C. P. Serine Phosphorylation and Negative Regulation of Stat3 by JNK. *Journal of Biological Chemistry* **274,** 31055–31061 (1999).

43. Turkson, J. *et al.* Requirement for Ras/Rac1-mediated p38 and c-Jun N-terminal kinase signaling in Stat3 transcriptional activity induced by the Src oncoprotein. *Molecular and cellular biology* **19,** 7519–28 (1999).

44. Kovarik, P. *et al.* Stress-induced phosphorylation of STAT1 at Ser727 requires p38 mitogen-activated protein kinase whereas IFN-gamma uses a different signaling pathway. *Proceedings of the National Academy of Sciences of the United States of America* **96,** 13956–61 (1999).

45. Battle, T. E., Lynch, R. a & Frank, D. a. Signal transducer and activator of transcription 1 activation in endothelial cells is a negative regulator of angiogenesis. *Cancer research* **66,** 3649–57 (2006).

46. Chen, Z. & Han, Z. C. STAT3: a critical transcription activator in angiogenesis. *Medicinal research reviews* **28,** 185–200 (2008).

47. Haspel, R. L. & Darnell, J. E. A nuclear protein tyrosine phosphatase is required for the inactivation of Stat1. *Proceedings of the National Academy of Sciences of the United States of America* **96,** 10188–93 (1999).

48. Wu, T. R. *et al.* SHP-2 is a dual-specificity phosphatase involved in Stat1 dephosphorylation at both tyrosine and serine residues in nuclei. *The Journal of biological chemistry* **277,** 47572–80 (2002).

49. Shuai, K. & Liu, B. Regulation of JAK-STAT signalling in the immune system. *Nature reviews. Immunology* **3,** 900–11 (2003).

50. Endo, T. a *et al.* A new protein containing an SH2 domain that inhibits JAK kinases. *Nature* **387,** 921–4 (1997).

51. Paukku, K. & Silvennoinen, O. STATs as critical mediators of signal transduction and transcription: lessons learned from STAT5. *Cytokine & growth factor reviews* **15,** 435–55 (2004).

52. Hennighausen, L. & Robinson, G. Interpretation of cytokine signaling through the transcription factors STAT5A and STAT5B. *Genes & development* **22,** 711–721 (2008).

53. Yang, X., Qiao, D., Meyer, K. & Friedl, A. Signal transducers and activators of transcription mediate fibroblast growth factor-induced vascular endothelial morphogenesis. *Cancer Research* **69,** 1668–1677 (2009).

54. Yang, X. *et al.* Angiogenesis induced by signal transducer and activator of transcription 5A (STAT5A) is dependent on autocrine activity of proliferin. *The Journal of biological chemistry* **287,** 6490–502 (2012).

55. Yanai, H., Negishi, H. & Taniguchi, T. Inception , impact and implications in oncogenesis The IRF family of transcription factors. **1,** 1376–1386 (2012).

56. Chen, H. & Jiang, Z. The essential adaptors of innate immune signaling. *Protein & cell* **4,** 27–39 (2013).

57. Kröger, A., Köster, M., Schroeder, K., Hauser, H. & Mueller, P. P. Activities of IRF-1. *Journal of interferon & cytokine research : the official journal of the International Society for Interferon and Cytokine Research* **22,** 5–14 (2002).

58. Guenzi, E. *et al.* The guanylate binding protein-1 GTPase controls the invasive and angiogenic capability of endothelial cells through inhibition of MMP-1 expression. *The EMBO journal* **22,** 3772–82 (2003).

59. Abdullah, N., Balakumari, M. & Sau, A. K. Dimerization and its role in GMP formation by human guanylate binding proteins. *Biophysical journal* **99,** 2235–44 (2010).

60. Vestal, D. J. The guanylate-binding proteins (GBPs): proinflammatory cytokine-induced members of the dynamin superfamily with unique GTPase activity. *Journal of interferon & cytokine research : the official journal of the International Society for Interferon and Cytokine Research* **25,** 435–43 (2005).

61. Vestal, D. J. & Jeyaratnam, J. a. The guanylate-binding proteins: emerging insights into the biochemical properties and functions of this family of large interferon-induced guanosine triphosphatase. *Journal of interferon & cytokine research : the official journal of the International Society for Interferon and Cytokine Research* **31,** 89–97 (2011).

62. Abdullah, N., Srinivasan, B., Modiano, N., Cresswell, P. & Sau, A. K. Role of individual domains and identification of internal gap in human guanylate binding protein-1. *Journal of molecular biology* **386,** 690–703 (2009).

63. Tripal, P. *et al.* Unique features of different members of the human guanylate-binding protein family. *Journal of interferon & cytokine research : the official journal of the International Society for Interferon and Cytokine Research* **27,** 44–52 (2007).

64. Staton, C. a, Reed, M. W. R. & Brown, N. J. A critical analysis of current in vitro and in vivo angiogenesis assays. *International journal of experimental pathology* **90,** 195–221 (2009).

65. Auerbach, R., Lewis, R., Shinners, B., Kubai, L. & Akhtar, N. Angiogenesis assays: a critical overview. *Clinical chemistry* **49,** 32–40 (2003).

66. Korff, T. & Augustin, H. G. Tensional forces in fibrillar extracellular matrices control directional capillary sprouting. *Journal of cell science* **112 (Pt 1,** 3249–58 (1999).

67. Arnaoutova, I. & Kleinman, H. K. In vitro angiogenesis: endothelial cell tube formation on gelled basement membrane extract. *Nature protocols* **5,** 628–35 (2010).

68. Stahl, A. *et al.* The mouse retina as an angiogenesis model. *Investigative ophthalmology & visual science* **51,** 2813–26 (2010).

69. Fruttiger, M. Development of the retinal vasculature. *Angiogenesis* **10,** 77–88 (2007).

70. Gerhardt, H. *et al.* VEGF guides angiogenic sprouting utilizing endothelial tip cell filopodia. *The Journal of cell biology* **161,** 1163–77 (2003).

71. Wen, Z., Zhong, Z. & Darnell, J. E. Maximal activation of transcription by Stat1 and Stat3 requires both tyrosine and serine phosphorylation. *Cell* **82,** 241–50 (1995).

72. Suslov, O. & Steindler, D. a. PCR inhibition by reverse transcriptase leads to an overestimation of amplification efficiency. *Nucleic acids research* **33,** e181 (2005).

73. Pfaffl, M. W. A new mathematical model for relative quantification in real-time RT-PCR. *Nucleic acids research* **29,** e45 (2001).

74. Ramsauer, K. *et al.* Distinct modes of action applied by transcription factors STAT1 and IRF1 to initiate transcription of the IFN-gamma-inducible gbp2 gene. *Proceedings of the National Academy of Sciences of the United States of America* **104,** 2849–54 (2007).

75. Lee, J. H., Chun, T., Park, S.-Y. & Rho, S. B. Interferon regulatory factor-1 (IRF-1) regulates VEGF-induced angiogenesis in HUVECs. *Biochimica et biophysica acta* **1783,** 1654–62 (2008).

76. Britzen-Laurent, N. *et al.* GBP-1 acts as a tumor suppressor in colorectal cancer cells. *Carcinogenesis* **34,** 153–162 (2013).

77. Kovarik, P., Mangold, M. & Ramsauer, K. Specificity of signaling by STAT1 depends on SH2 and C-terminal domains that regulate Ser727 phosphorylation, differentially affecting specific target gene expression. *The EMBO journal* **20,** 91–100 (2001).

78. Lucas, S., Ghilardi, N., Li, J. & de Sauvage, F. J. IL-27 regulates IL-12 responsiveness of naive CD4+ T cells through Stat1-dependent and -independent mechanisms. *Proceedings of the National Academy of Sciences of the United States of America* **100,** 15047–52 (2003).

79. Yahata, Y. *et al.* Nuclear translocation of phosphorylated STAT3 is essential for vascular endothelial growth factor-induced human dermal microvascular endothelial cell migration and tube formation. *The Journal of Biological Chemistry* **278,** 40026–40031 (2003).

80. Ferrari, G. *et al.* TGF-β1 induces endothelial cell apoptosis by shifting VEGF activation of p38(MAPK) from the prosurvival p38β to proapoptotic p38α. *Molecular cancer research : MCR* **10,** 605–14 (2012).

81. Sundarrajan, M., Boyle, D. L., Chabaud-Riou, M., Hammaker, D. & Firestein, G. S. Expression of the MAPK kinases MKK-4 and MKK-7 in rheumatoid arthritis and their role as key regulators of JNK. *Arthritis and rheumatism* **48,** 2450–60 (2003).

82. Balasubramanian, S. *et al.* The interferon-gamma-induced GTPase, mGBP-2, inhibits tumor necrosis factor alpha (TNF-alpha) induction of matrix metalloproteinase-9 (MMP-9) by inhibiting NF-kappaB and Rac protein. *The Journal of biological chemistry* **286,** 20054–64 (2011).

Appendix

Appendix 1

Table 6:Primers pairs used in Q-PCR to amplify cDNA sequence of p38α and GAPDH.

Abreviation	Gene Name and Accesion number	Sequence (5' – 3')	Amplicon size (base pair)	Intron size	Anneling Temperature (°C)
p38α	p38 alpha Mitogen Activated Protein Kinase (NM_139012.2)	Pair 1: F: CAGGGGCTGAGCTTTTGAAGAAAAT R: CAAGTCGACAGCCAGGGGA	128	6504	60
		Pair 2: F: TTTTAAGACTCGTTGGAACCCCAGG R: TTCTCCAGCAAGTCGACAGCC	157	6504	60
		Pair 3: F: CTCCTCAGAGTCTGCAAGAAACTAT R: AGGATCGGCCACTGGTTCA	217	4805	60
		Pair 4: F: AGGGGCTGAGCTTTTGAAGAAAAT R: AGTCGACAGCCAGGGGATTG	125	6504	60
GAPDH	Glyceraldehyde-3-Phosphate Dehydrogenase (NM_002046)	F: GGAAGGTGAAGGTCGGAGTCAA R: GATCTCGCTCCTGGAAGATGGT	240	1722	60 (but works well within a wide temperature range)

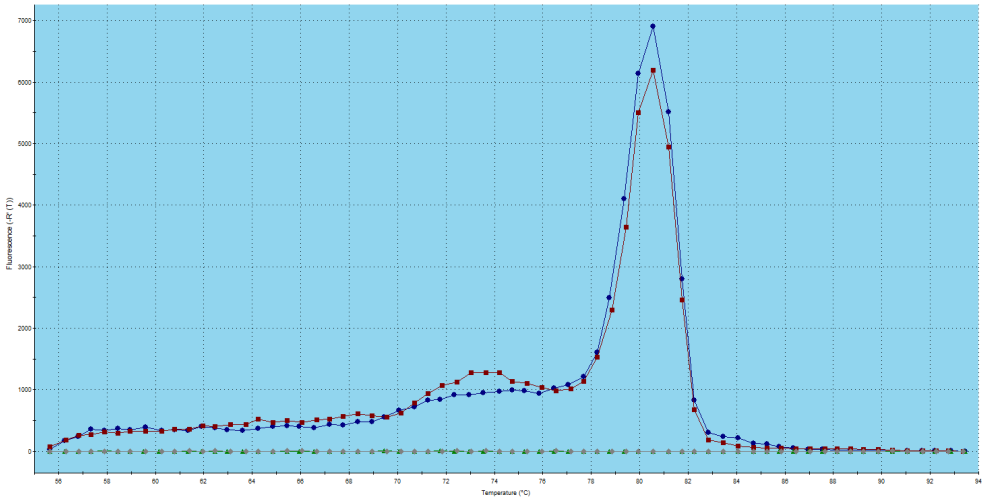

Figure 36: Melting Curve of p38α primer pair 1 (duplicates, lines blue and red) and pair 2 (flat line).

Appendix 2

Receptor of IL-27 is present in HUVEC.

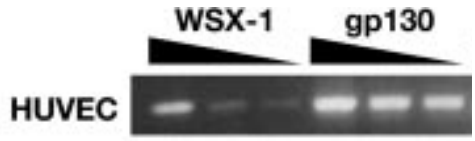

Figure 37: HUVEC respond to IL-27 stimulation. Total RNA was isolated from HUVEC and analyzed for expression of IL-27R subunits, WSX-1 and gp130, using serial dilutions (1:3) of cDNA templates by RT-PCR. Image withdrawal form Shimizu et al., 2006.

Appendix 3

After 24 hours stimulation with IL-27 is seen GBP1 and GBP2 expression in HUVEC (Figure 38). In Figure 39 is observed GBP1 and GBP2 reduced activation after STAT1 knockdown or IRF-1 knockdown (results from the lab).

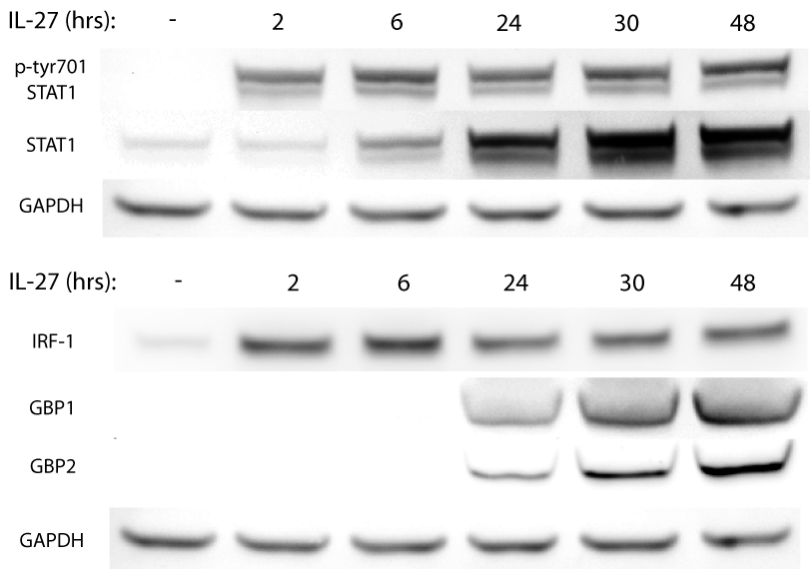

Figure 38: GBP1 and GBP2 are expressed after IL-27 stimulation. HUVEC were treated with IL-27 (20ng/mL) and cell lysis was performed at the time points shown. Cellular lysates were Immunobloted with antibodies used against phosphorylated STAT1 (Tyr701), Total STAT1, Total IRF-1, Total GBP1 and Total GBP2. GAPDH was used as loading control. Data are representative of three independent experiments.

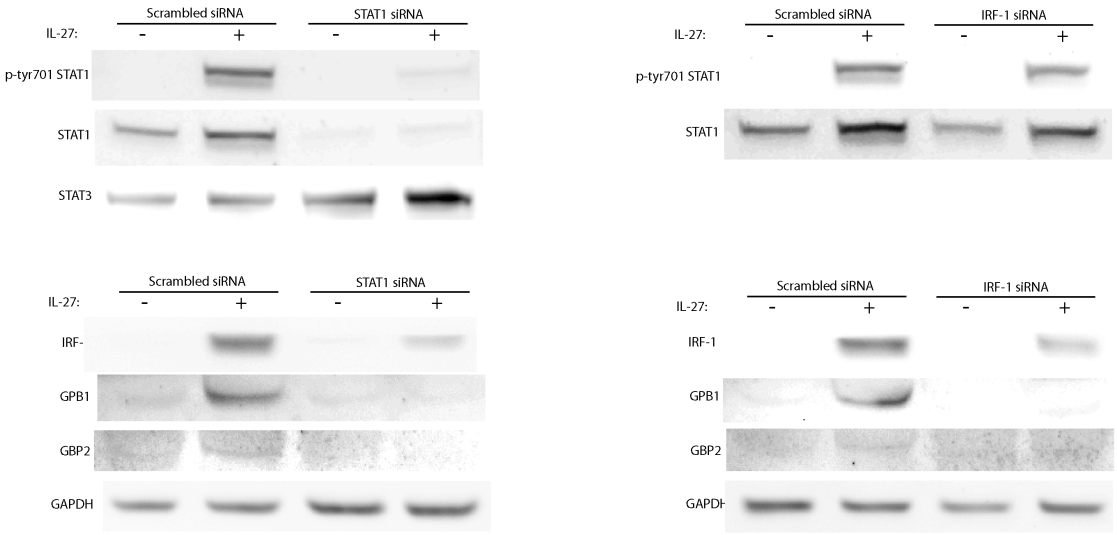

Figure 39: STAT1 and IRF-1 knockdown lead to reduced expression of both GBP1 and GBP2. Knockdown performed in EA.hy926 cell line, using Scrambled siRNA as control. Cells were stimulated for with IL-27 (20ng/mL) 6 hours and lysed by addition of cell lysis buffer. Cellular lysate was used for immunoblotting with antibody against phosphorylated STAT1 (Tyr701), Total STAT1, Total IRF-1 and Total GBP1 and GBP2. GAPDH was used as loading control. Data are representative of three independent experiments.